Electronic Supplementary Information

Interaction of *N*-Nitrosamines with Binuclear Copper Complexes for Luminescent Detection

Haosheng Feng,[a] Shao-Xiong Lennon Luo,[a] Robert G. Croy [b], John M. Essigmann[b] and Timothy M. Swager* [a]

[a]*Institute for Soldier Nanotechnologies and Department of Chemistry, Massachusetts Institute of Technology, 77 Massachusetts Avenue, Cambridge, MA, 02139, USA*

[b]*Department of Chemistry, Department of Biological Engineering and Center for Environmental Health Sciences, Massachusetts Institute of Technology, 77 Massachusetts Avenue, Cambridge, Massachusetts 02139, United States*

All original and processed data/metadata may be accessed at https://fairdomhub.org/studies/1140.

Table of Contents

1. NMR Spectra of Phosphines

1.1. Ph_2P(Pyrimidine) (1)

^{1}H NMR (500 MHz, $CDCl_3$)

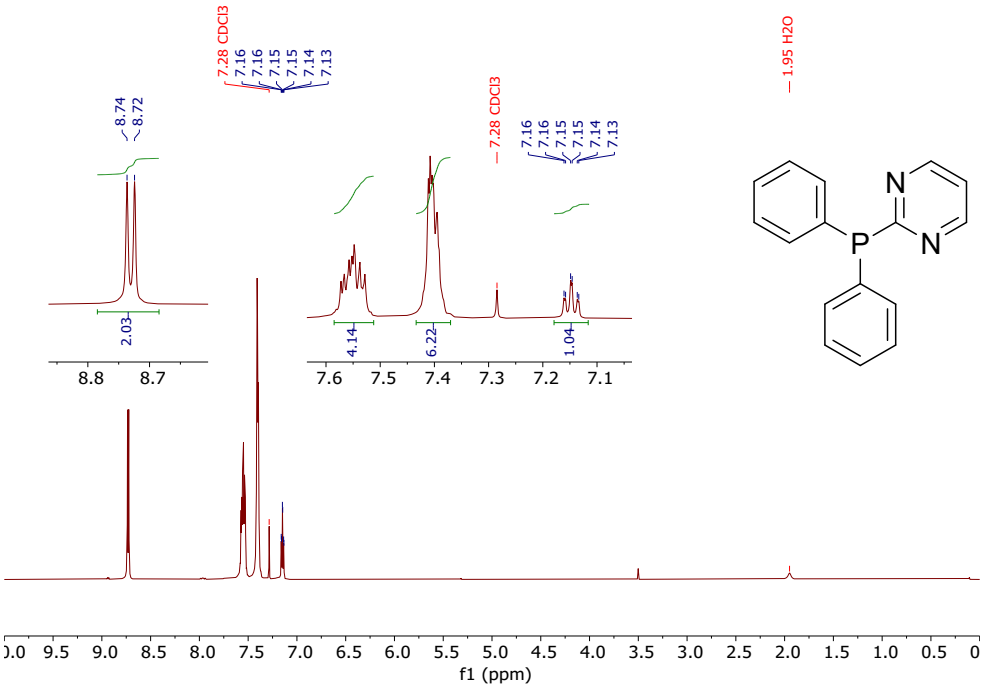

Figure S 1

^{31}P{^{1}H} NMR (202 MHz, $CDCl_3$)

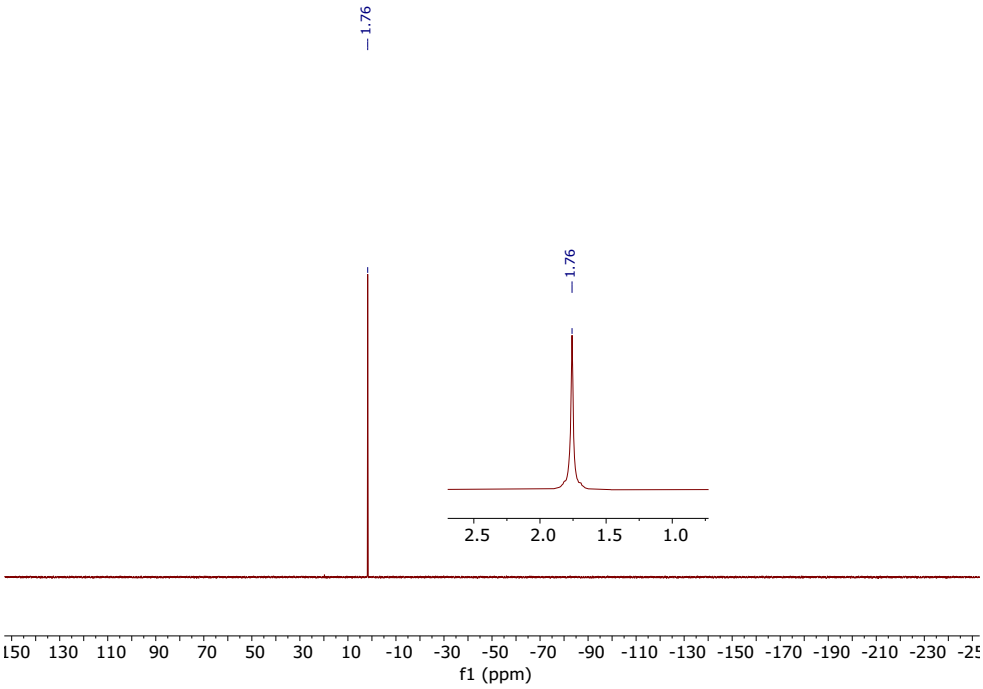

Figure S 2

1.2. Ph_2P(2-Quinazoline) (2)

^{1}H NMR (400 MHz, $CDCl_3$)

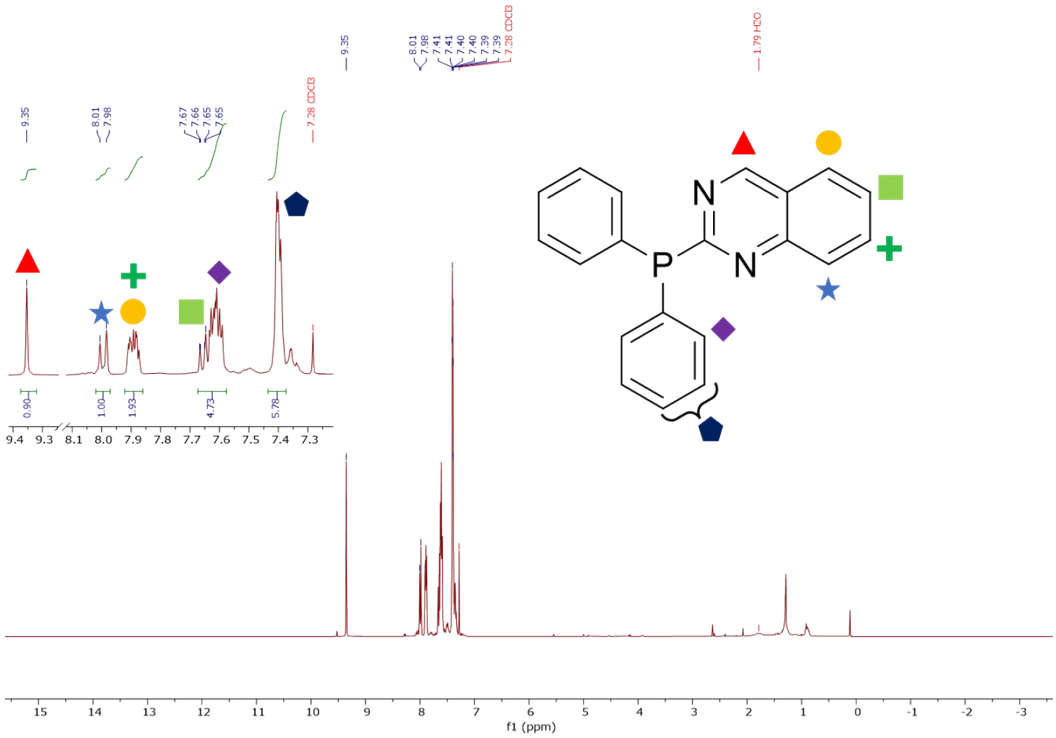

Figure S 3

^{31}P{^{1}H} NMR (162 MHz, $CDCl_3$)

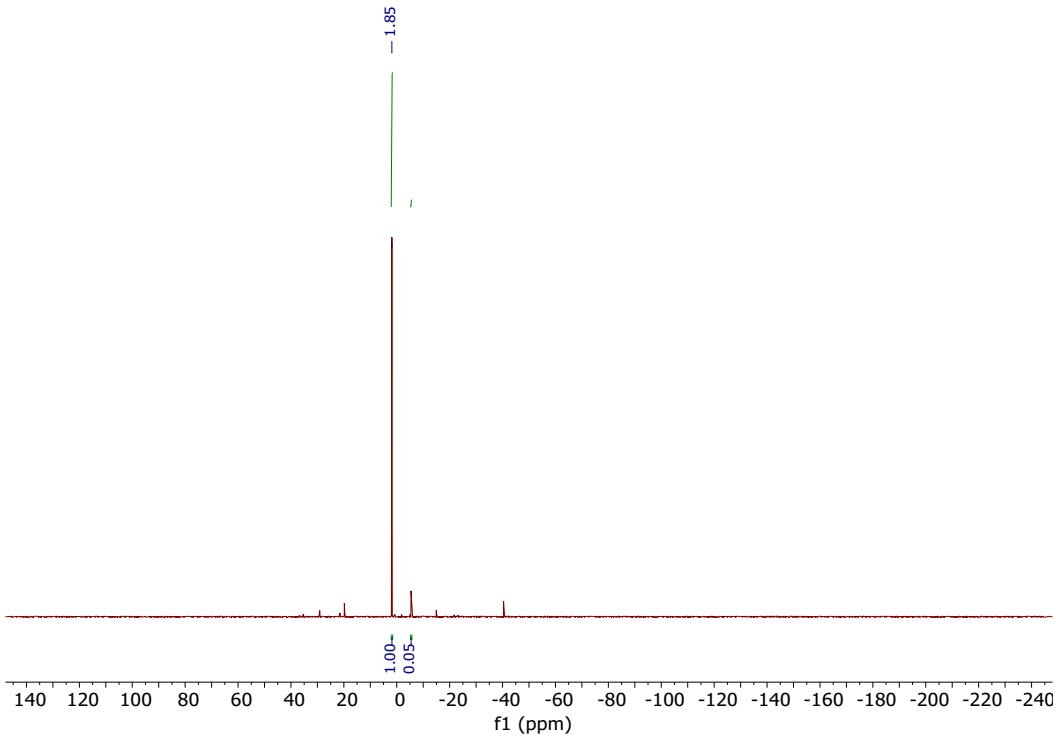

Figure S 4

^{1}H NMR COSY (400 MHz, $CDCl_3$)

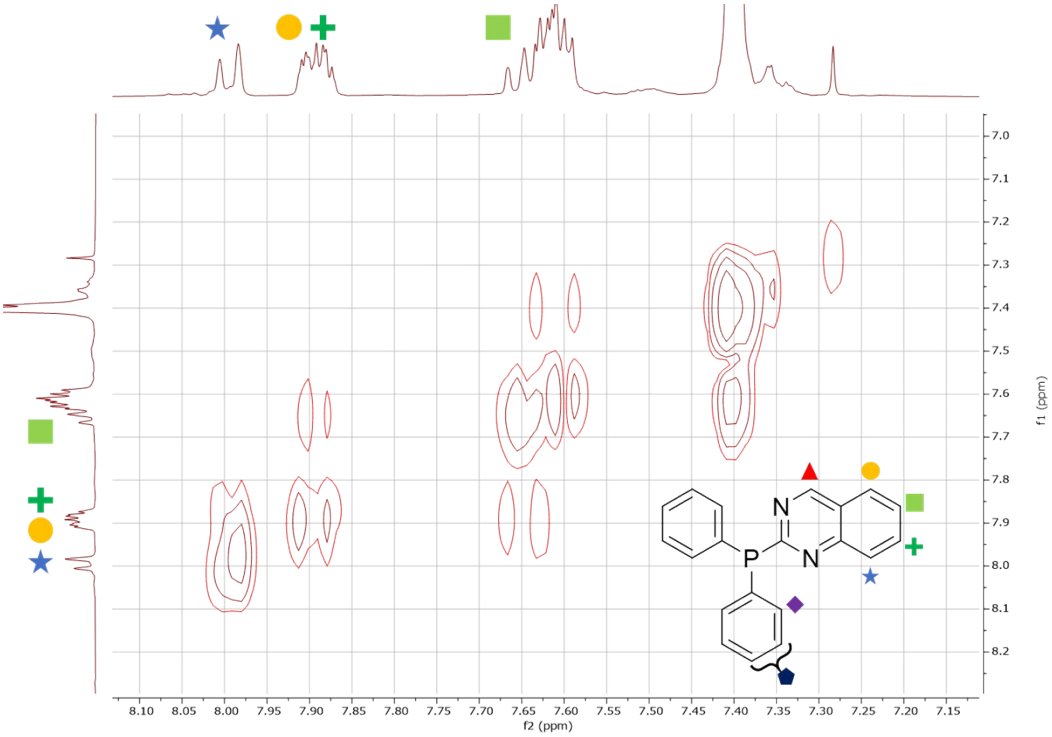

Figure S 5

^{1}H – ^{13}C HSQC (400 MHz, $CDCl_3$)

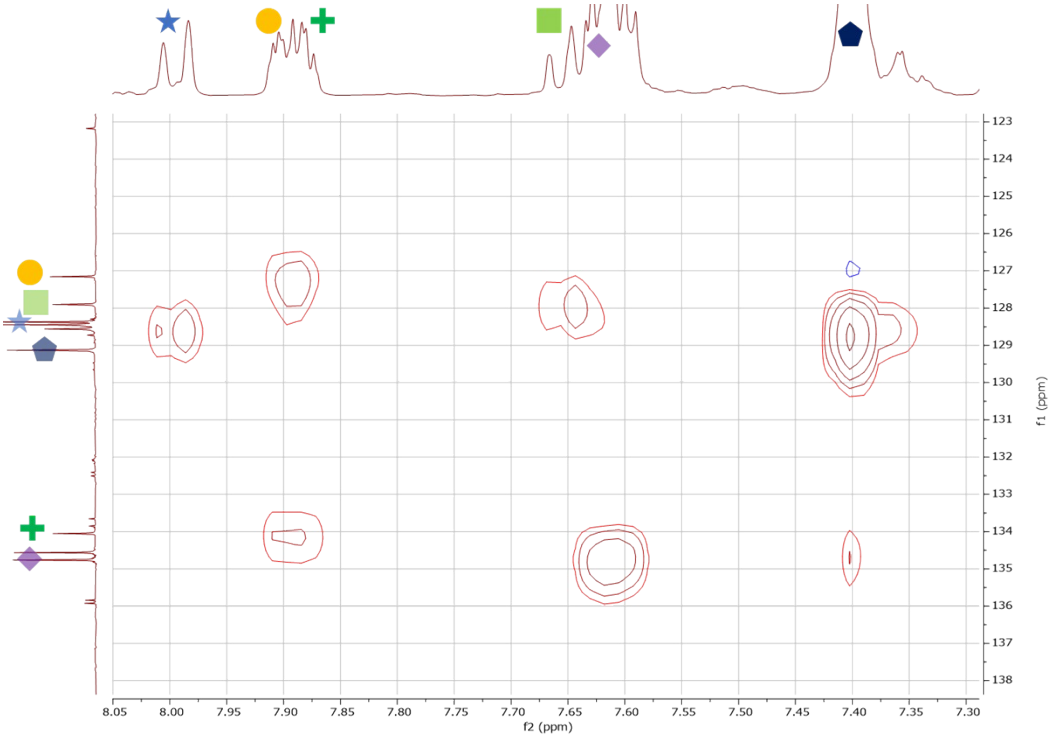

Figure S 6

^{1}H – ^{13}C HMBC (400 MHz, $CDCl_3$)

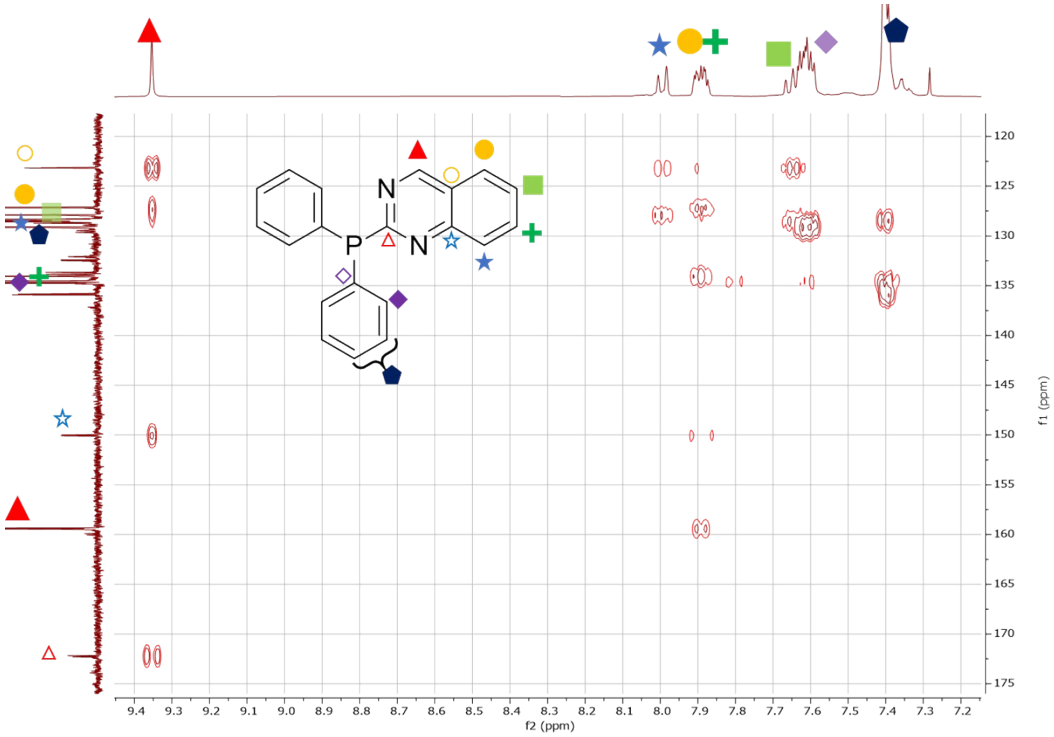

Figure S 7

$^{13}C\{^{1}H\}$ NMR (101 MHz, $CDCl_3$)

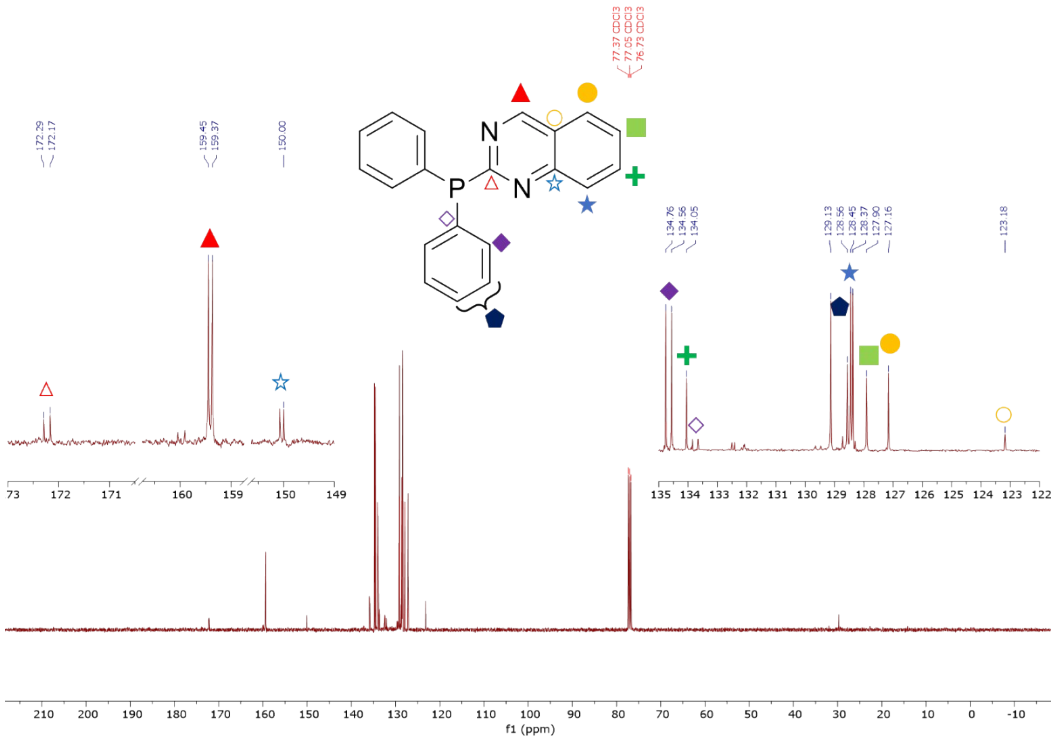

Figure S 8 Some carbon signals appear as doublets due to coupling to ^{31}P

1.3. Ph_2P(3-Isoquinoline) (3)

^{1}H NMR (500 MHz, $CDCl_3$)

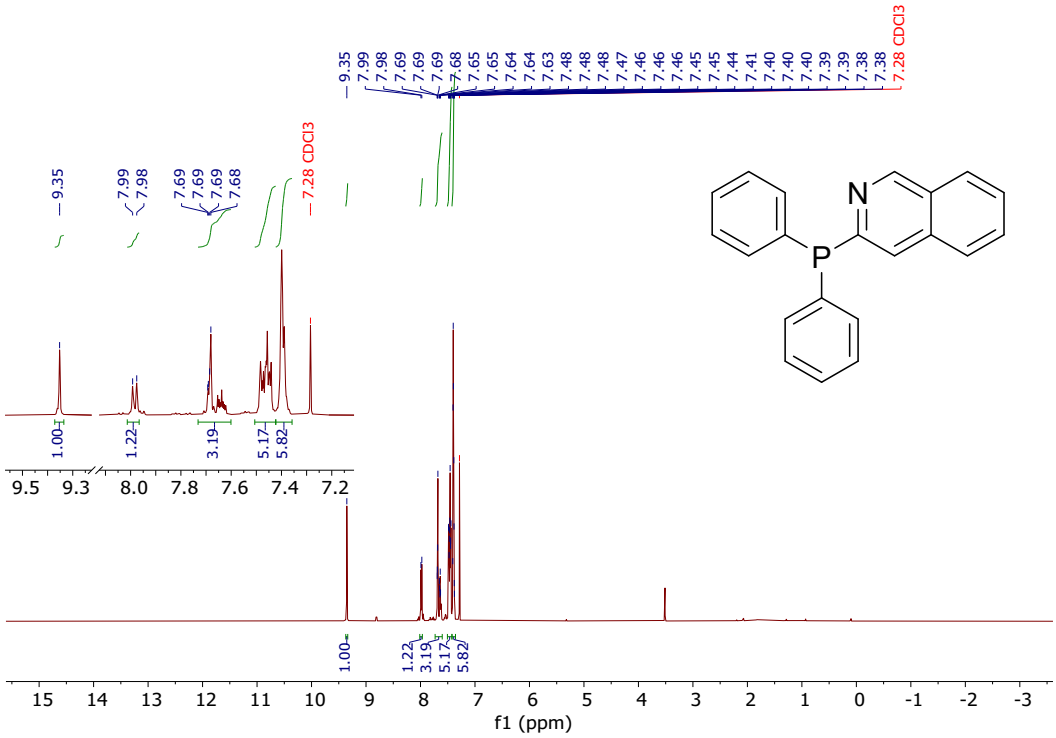

Figure S 9

^{31}P{^{1}H} NMR (203 MHz, $CDCl_3$)

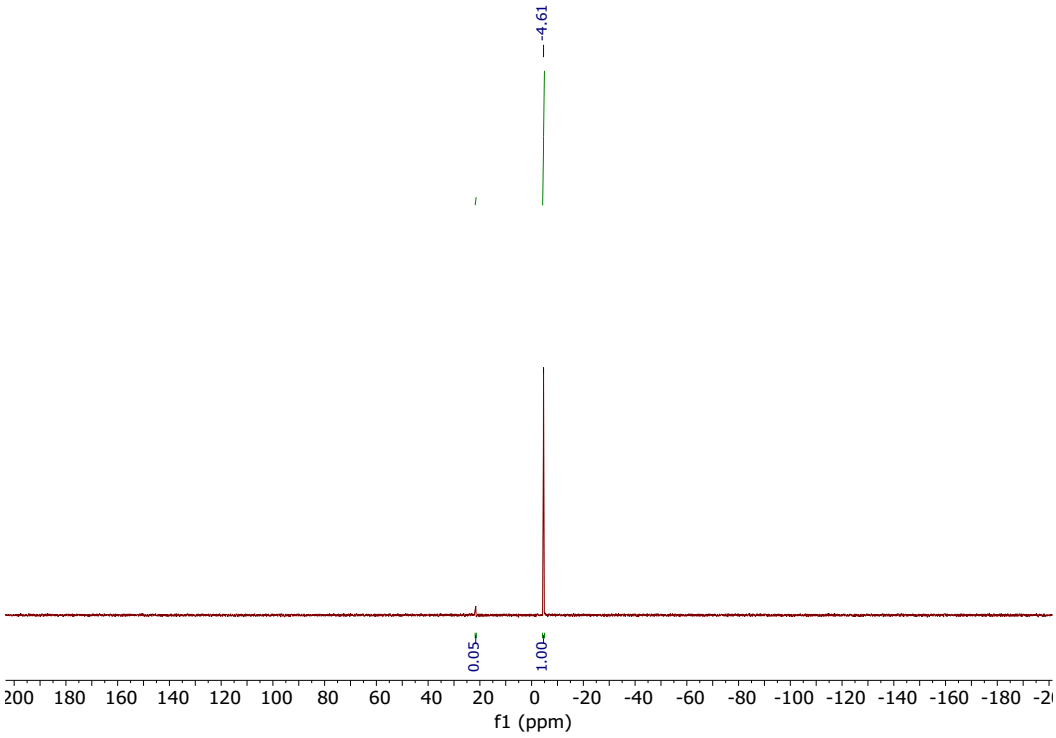

Figure S 10

$^{13}C\{^{1}H\}$ NMR (126 MHz, $CDCl_3$)

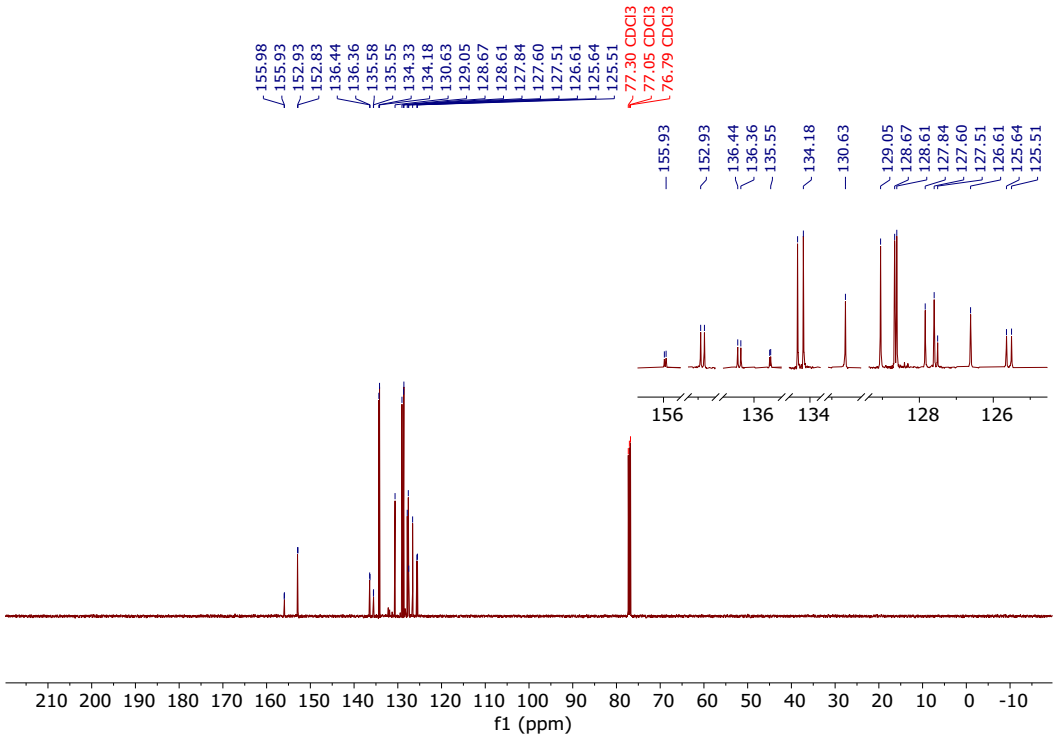

Figure S 11 Some carbon signals appear as doublets due to coupling to ^{31}P

1.4. Ph_2P(2-Quinoline) (4)

^{1}H NMR (500 MHz, $CDCl_3$)

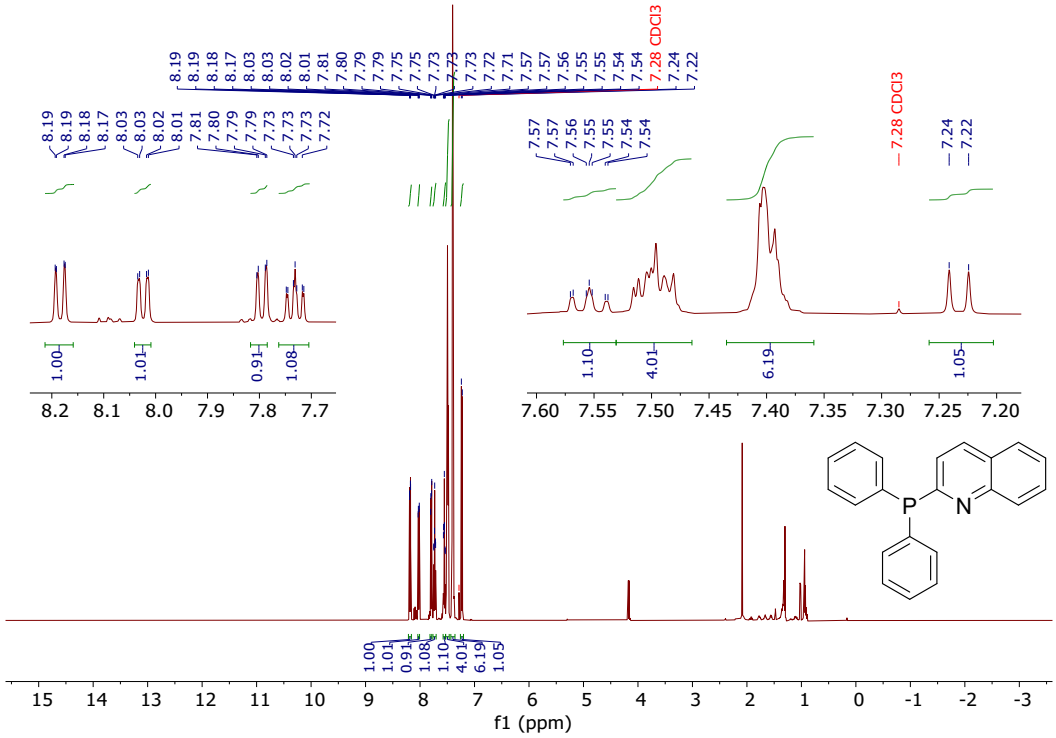

Figure S 12

^{31}P NMR (202 MHz, $CDCl_3$)

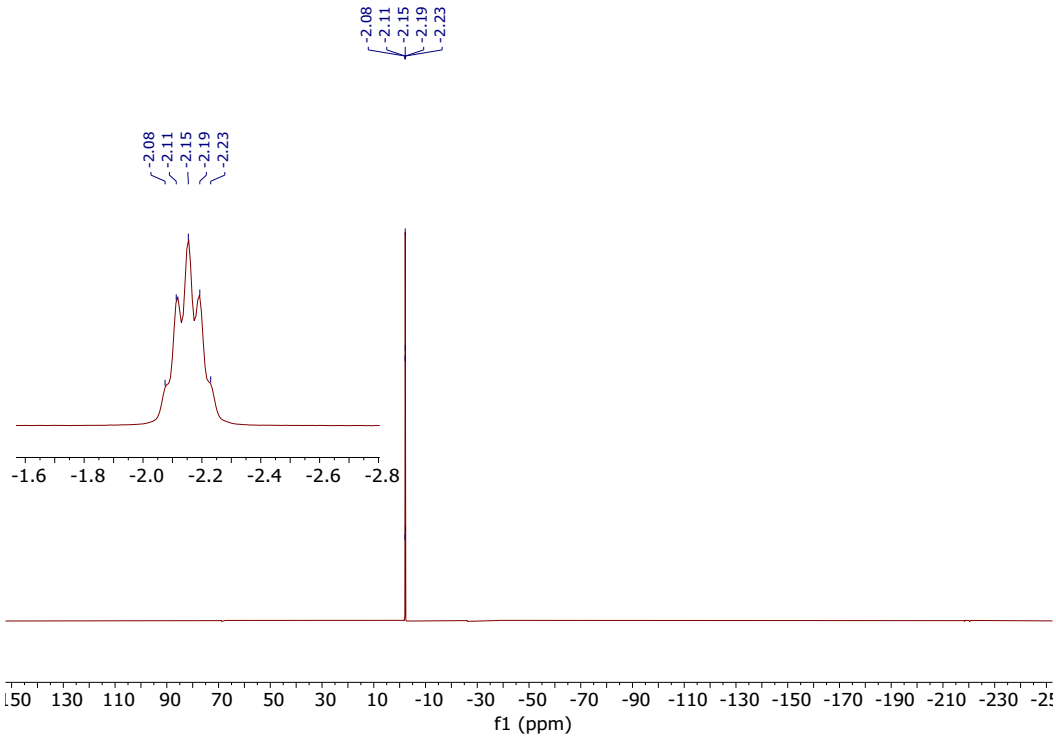

Figure S 13 Apparent quintet is due to coupling to ^{1}H

$^{13}C\{^{1}H\}$ NMR (125 MHz, $CDCl_3$)

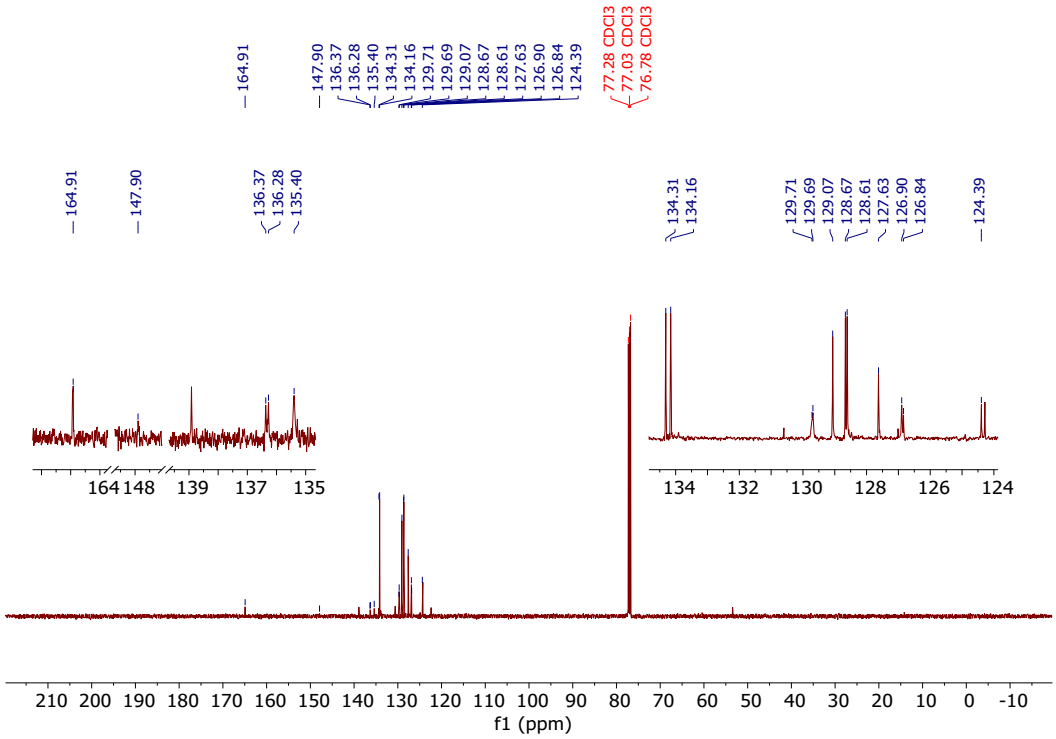

Figure S 14 Some carbon signals appear as doublets because of coupling to ^{31}P

1.5. Ph_2P(1-Isoquinoline) (5)

^{1}H NMR (400 MHz, $CDCl_3$)

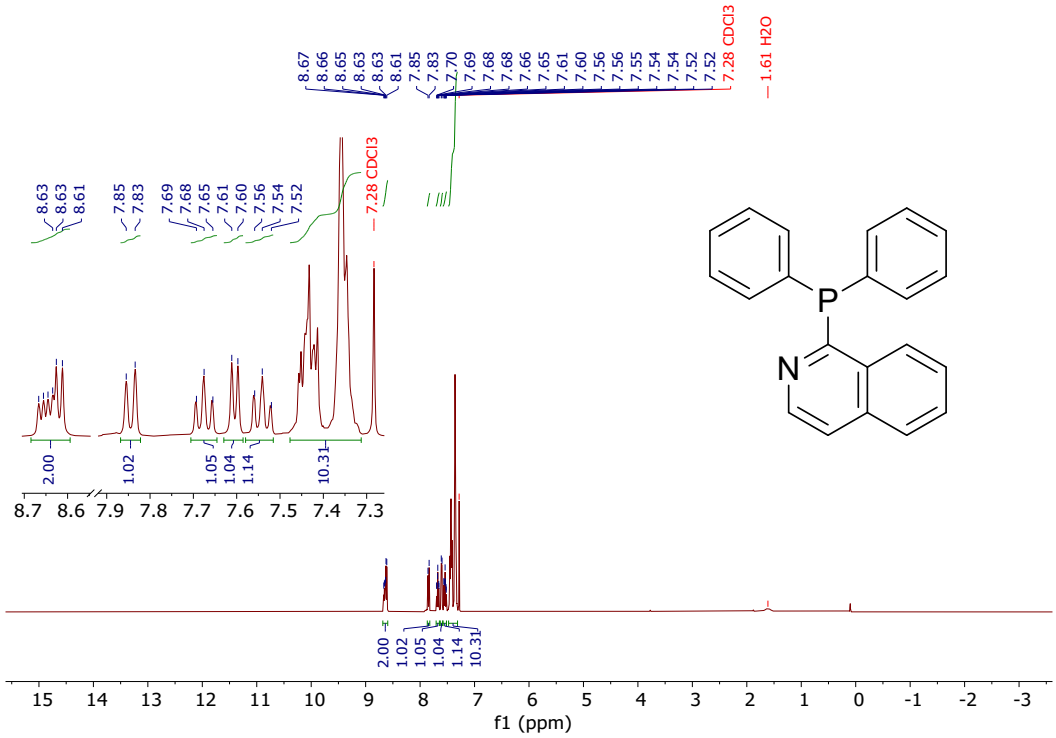

Figure S 15

^{31}P{^{1}H} NMR (162 MHz, $CDCl_3$)

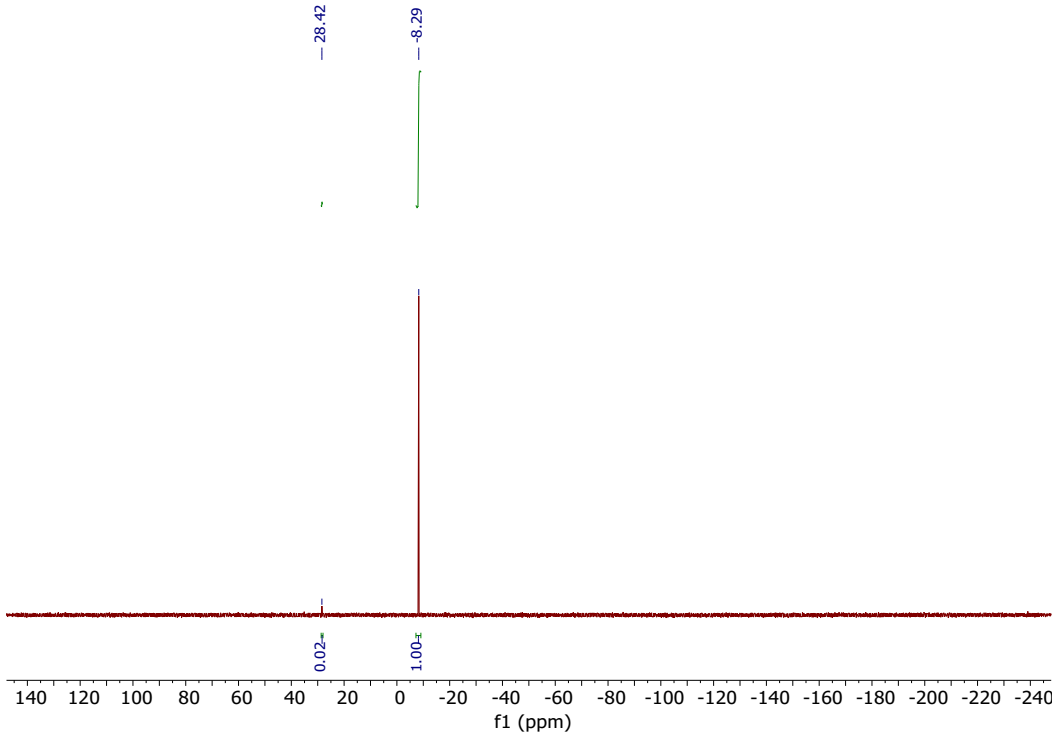

Figure S 16

$^{13}C\{^{1}H\}$ NMR (101 MHz, $CDCl_3$)

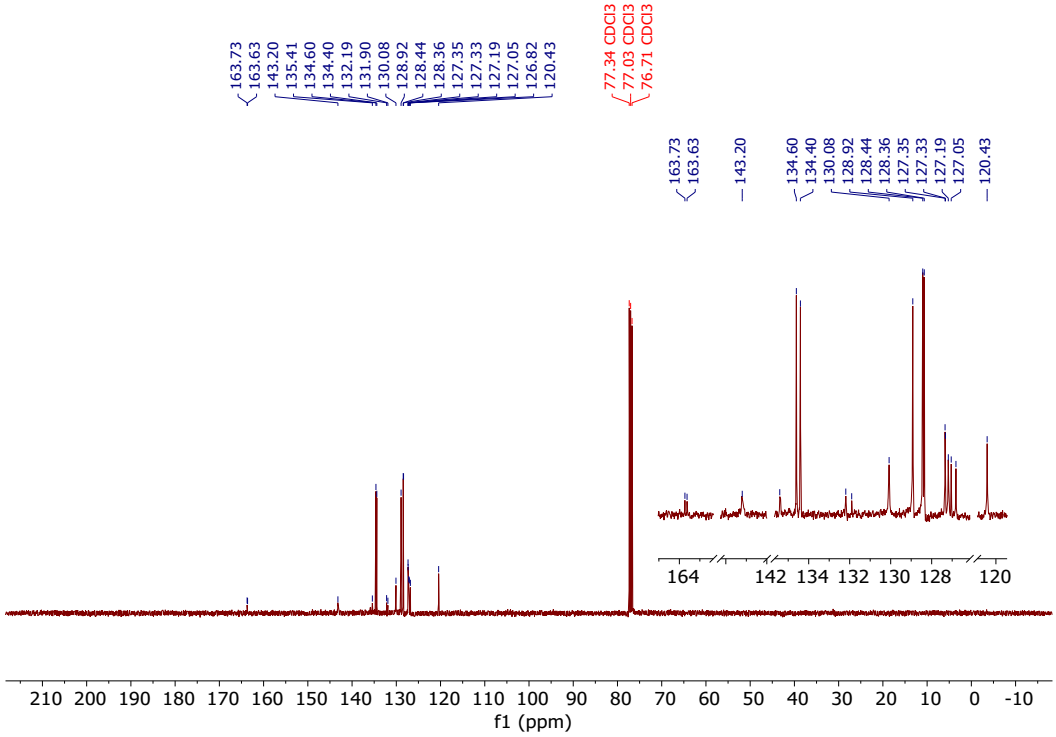

Figure S 17 Some carbon signals appear as doublets due to coupling to ^{31}P

1.6. Ph_2P(1-Isoquinoline) phosphine oxide (5-O)

^{1}H NMR (400 MHz, $CDCl_3$)

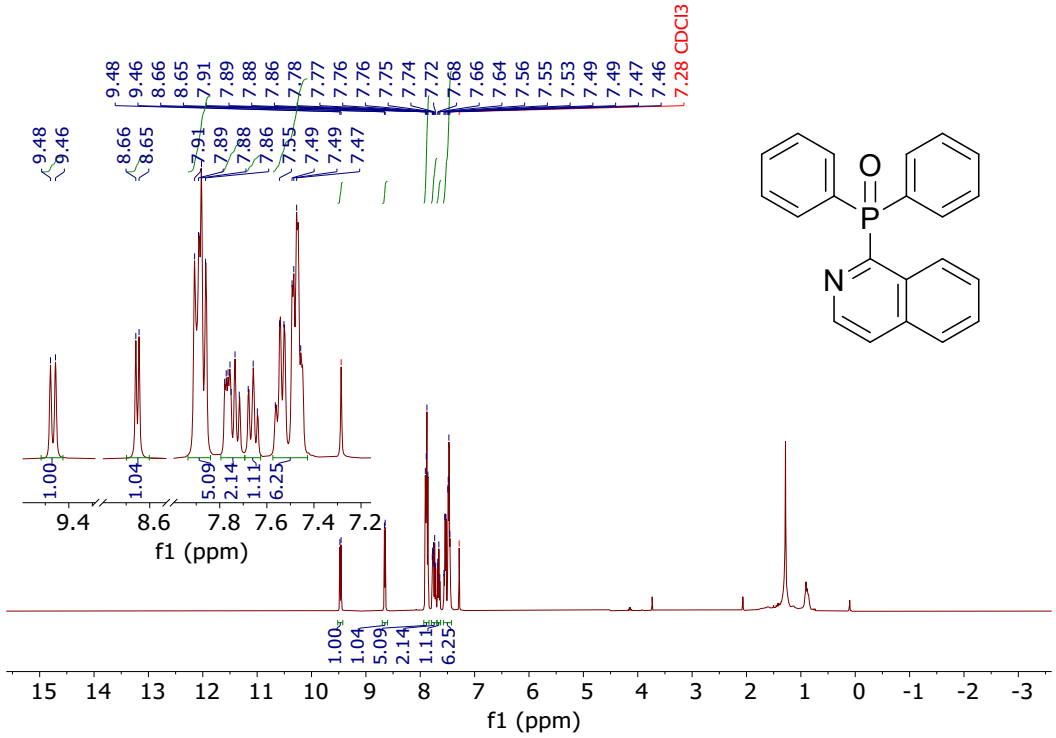

Figure S 18

$^{31}P\{^1H\}$ NMR (162 MHz, $CDCl_3$)

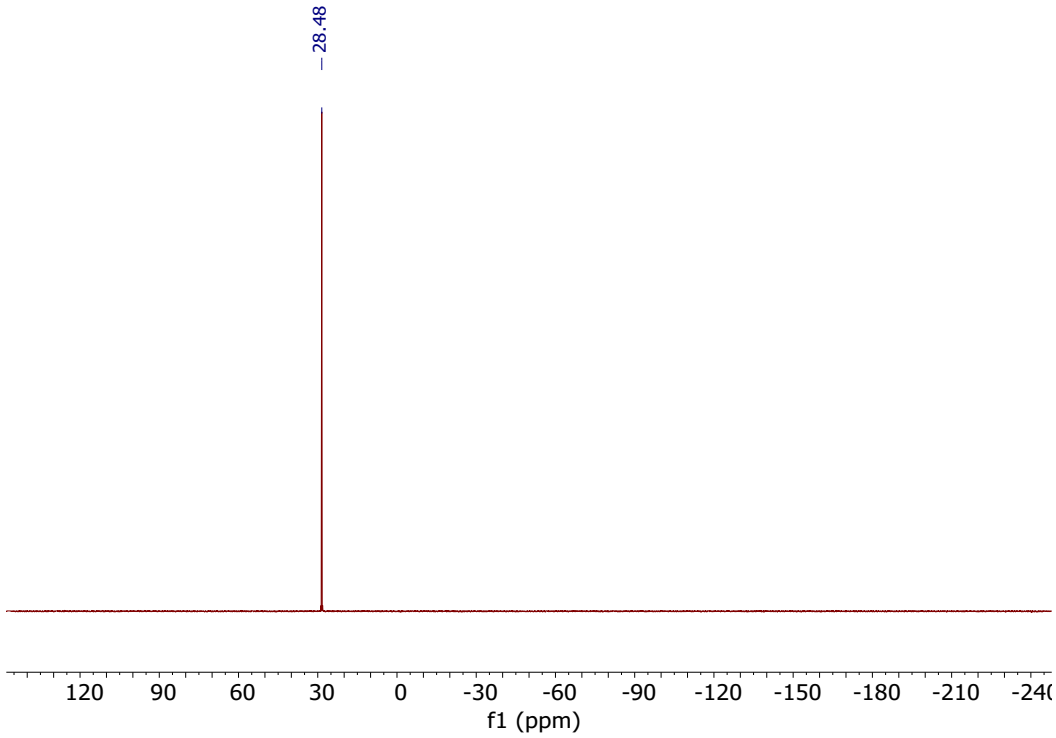

Figure S 19

2. NMR Spectra of Cu(I) Complexes

2.1. 1-Cu after recrystallizing from DCM – Et_2O

^{1}H NMR (500 MHz, MeOD)

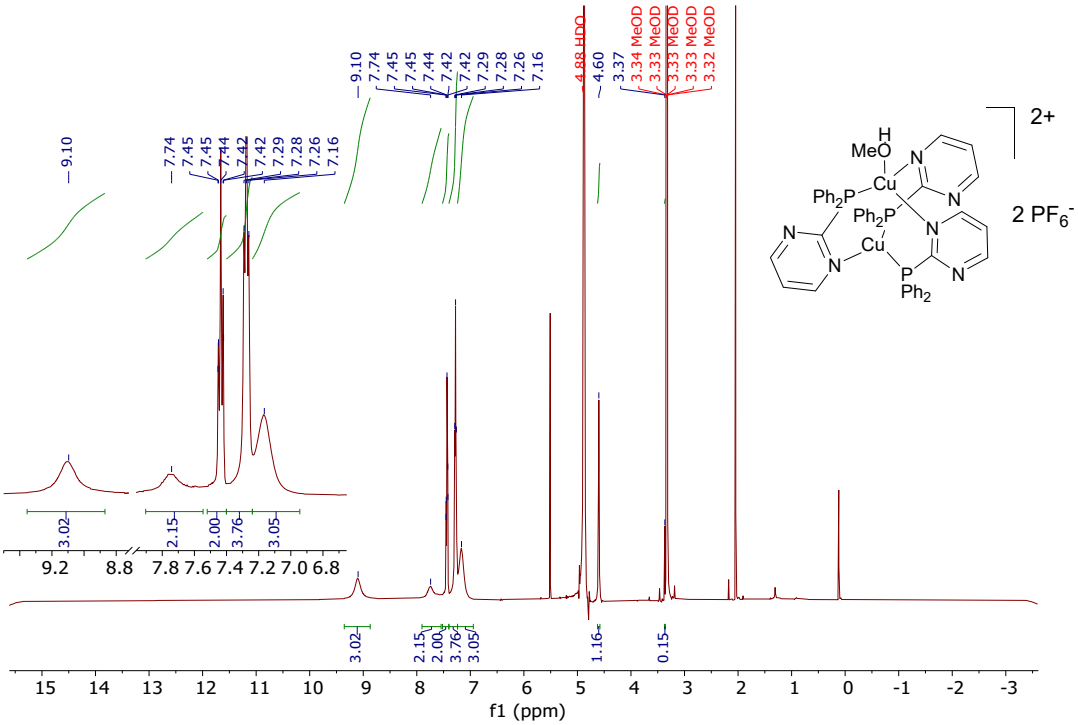

Figure S 20

^{31}P{^{1}H} NMR (202 MHz, $CDCl_3$)

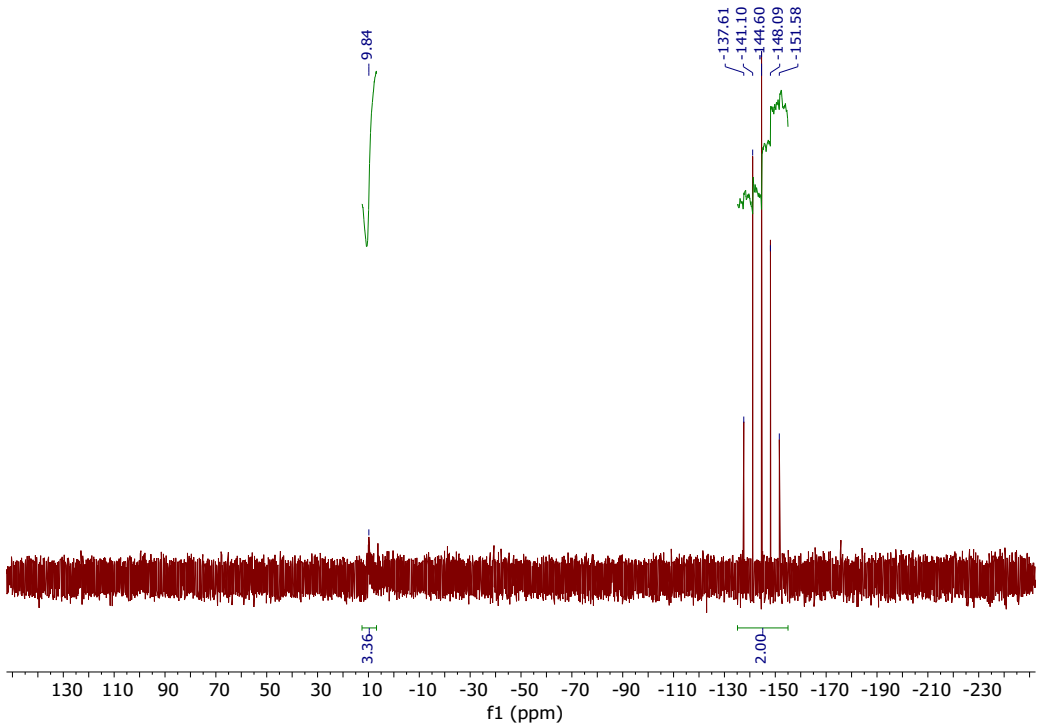

Figure S 21

^{19}F NMR (376 MHz, $CDCl_3$)

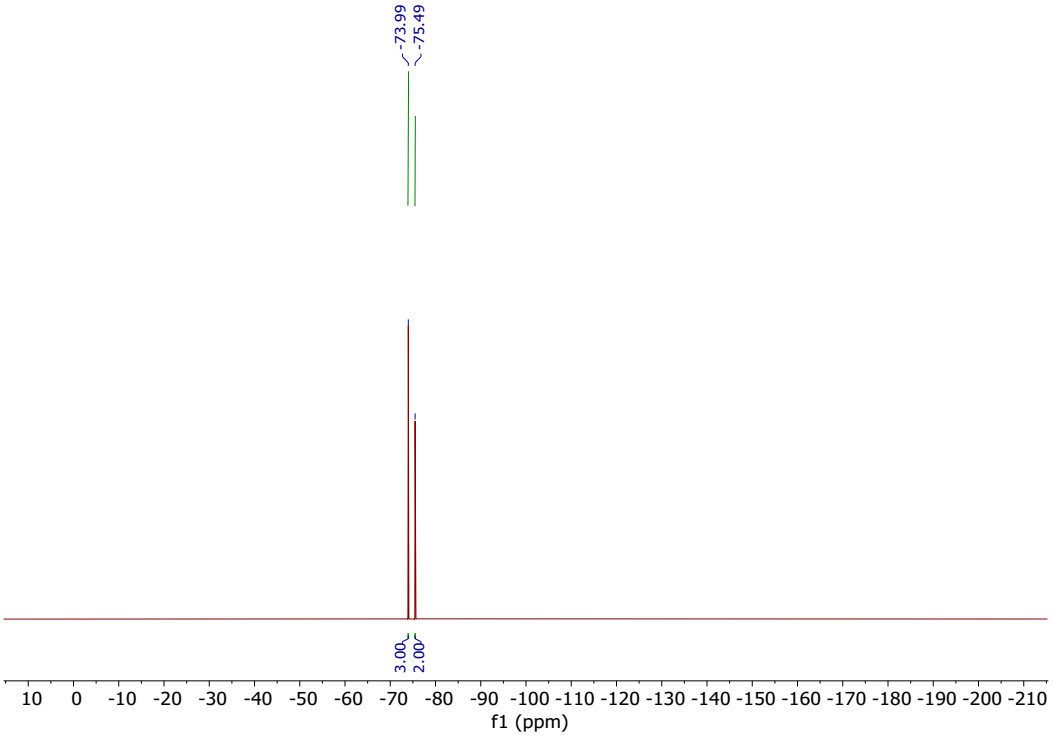

Figure S 22

2.2. 2-Cu after initial precipitation from reaction

^{1}H NMR (400 MHz, $CDCl_3$)

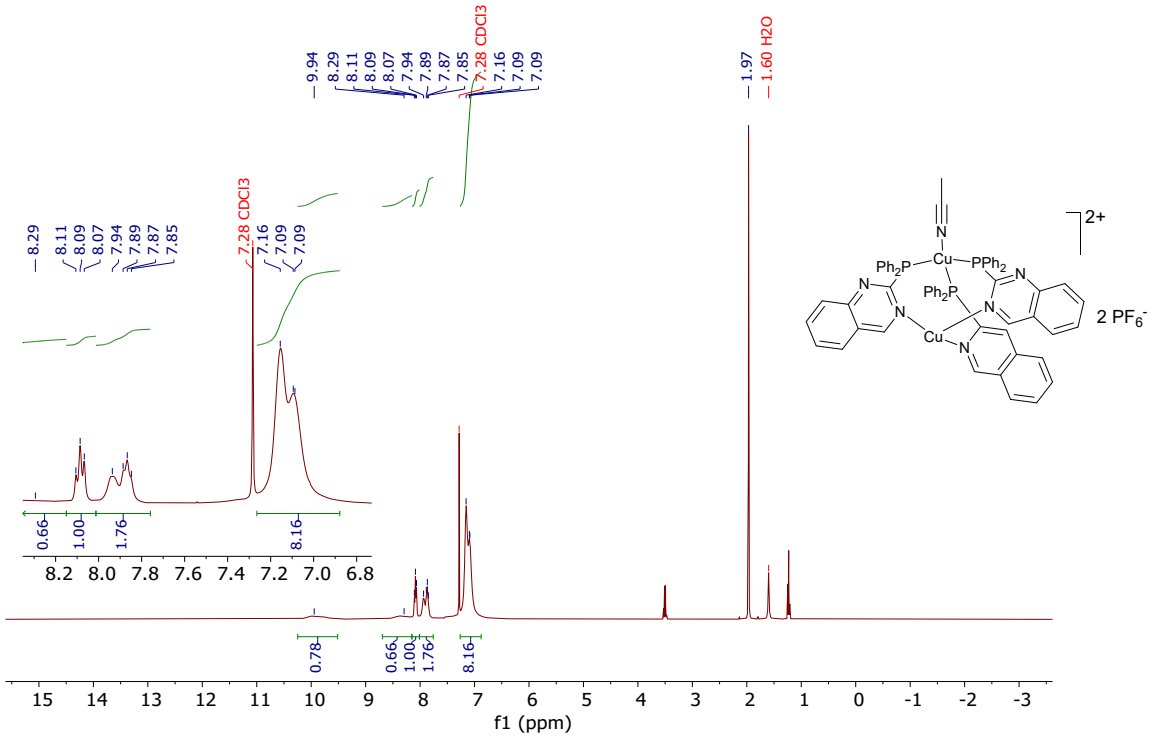

Figure S 23. Residual Et_2O is visible in the spectrum. Shown HH structure is postulated based on the singlet ^{31}P signal at 10.7 ppm.

^{13}C{^{1}H} NMR (100 MHz, $CDCl_3$)

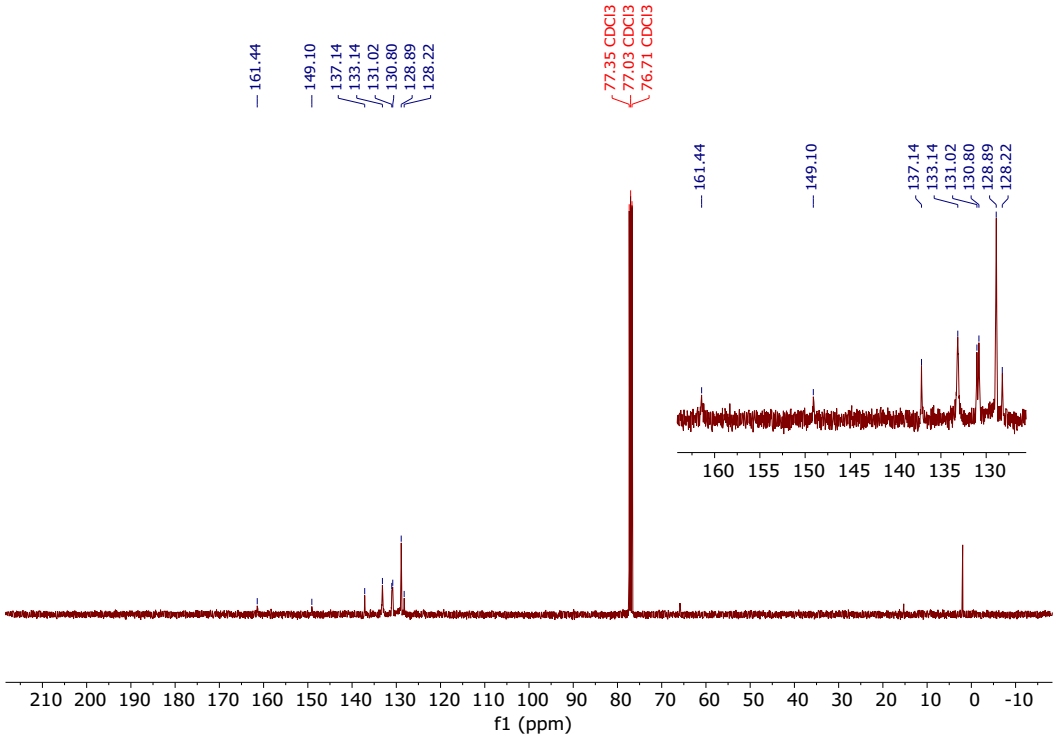

Figure S 24

$^{31}P\{^{1}H\}$ NMR (162 MHz, $CDCl_3$)

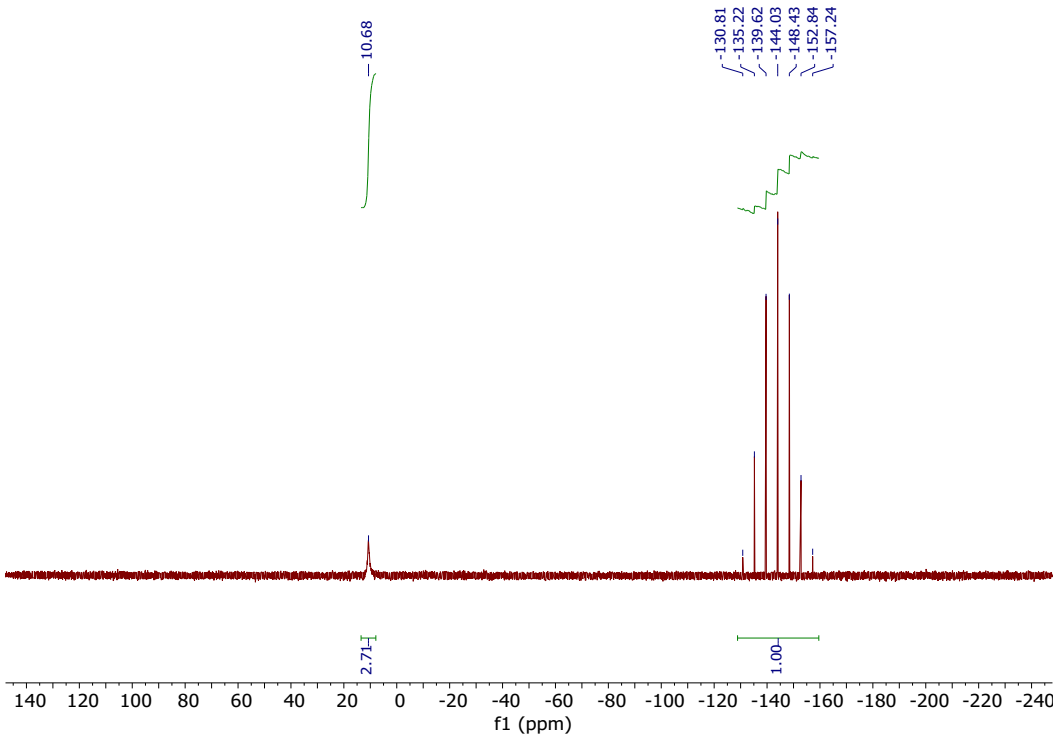

Figure S 25

2.3. 3-Cu after precipitation from reaction

^{1}H NMR (400 MHz, $CDCl_3$)

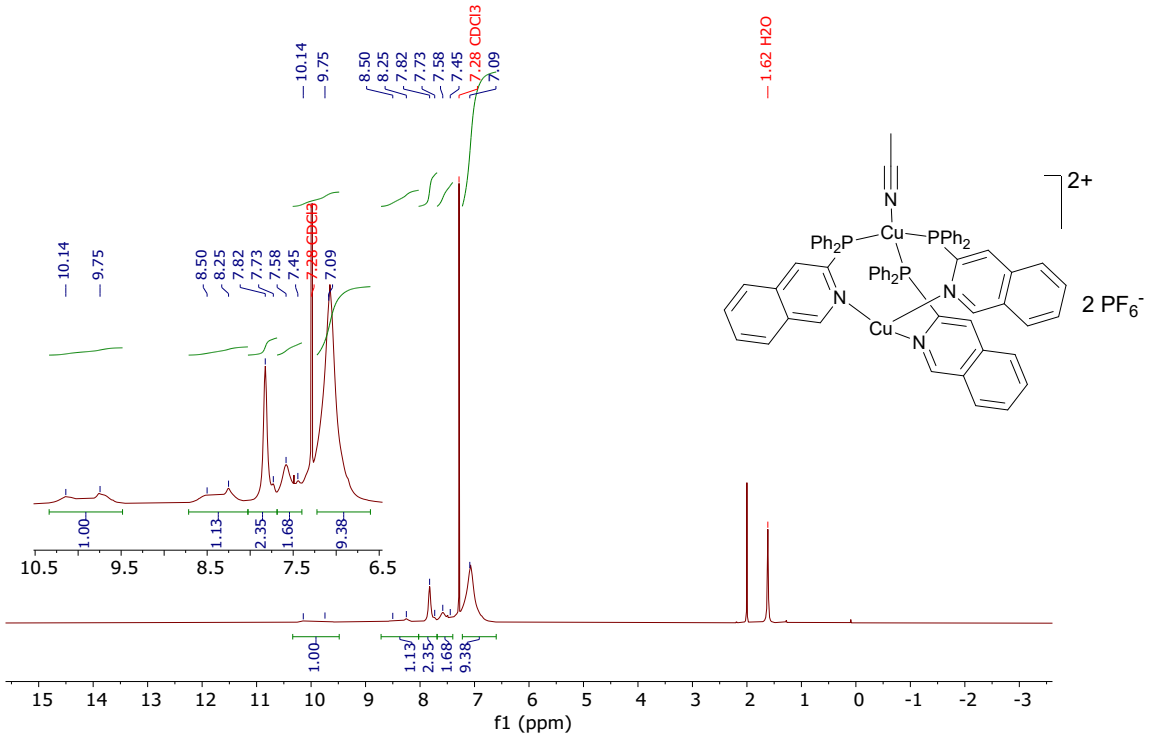

Figure S 26

^{13}C{^{1}H} NMR (100 MHz, $CDCl_3$)

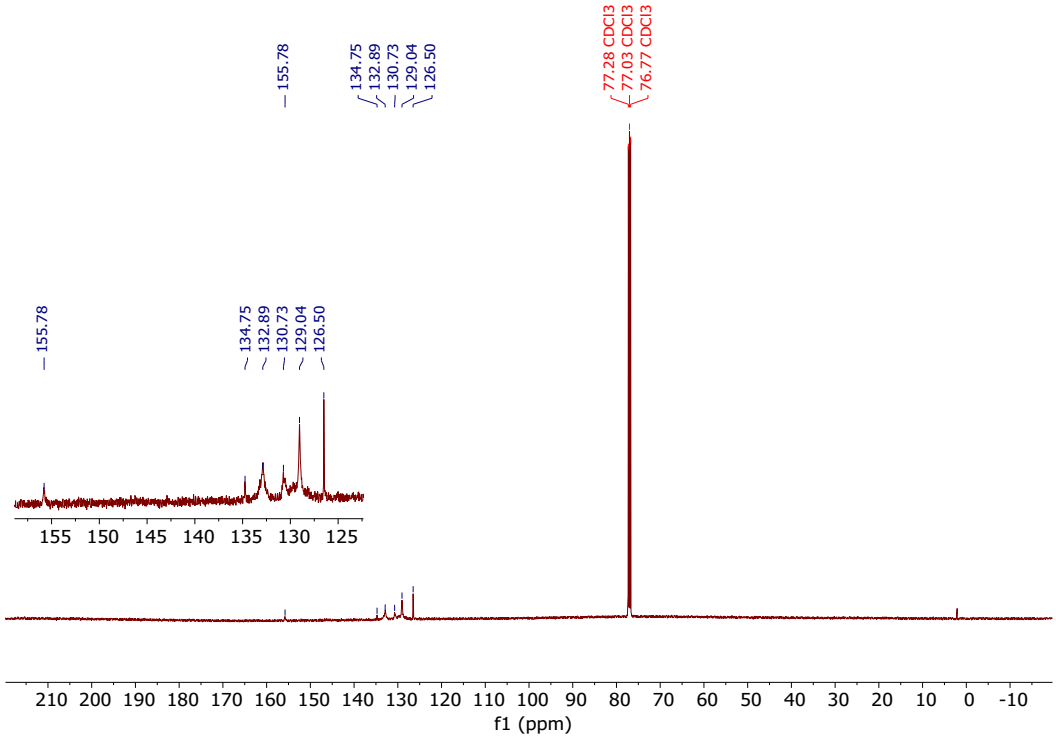

Figure S 27

$^{31}P\{^{1}H,^{19}F\}$ NMR (162 MHz, $CDCl_3$)

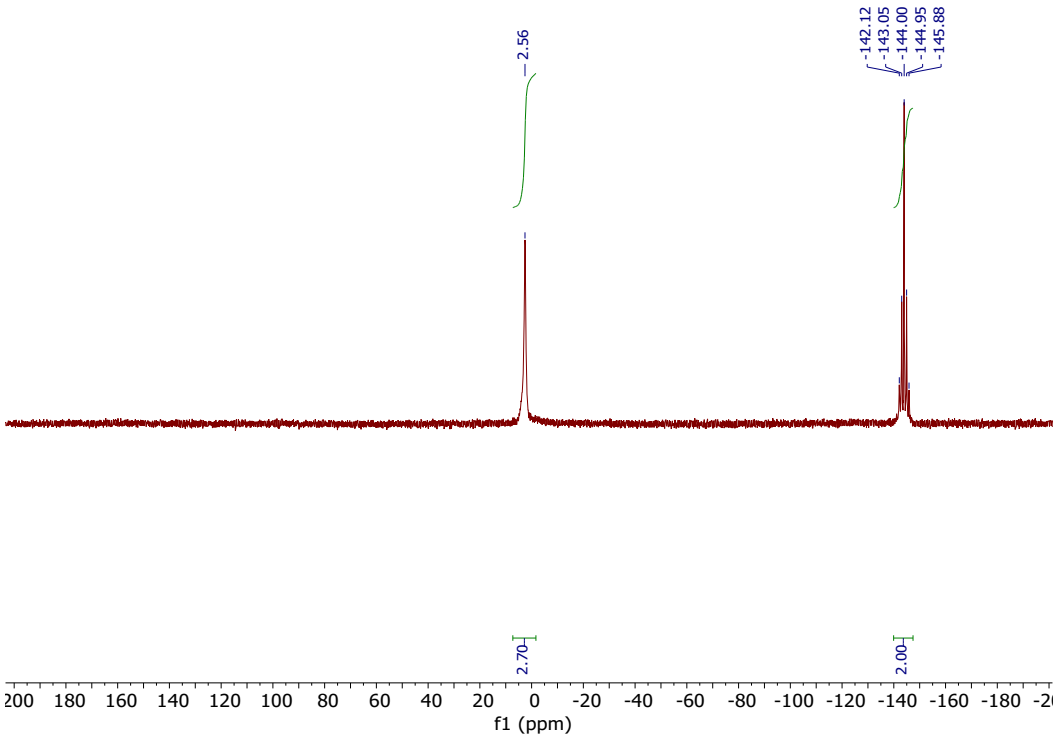

Figure S 28

2.4. 4-Cu after precipitation from reaction

^{1}H NMR (500 MHz, CD_3CN)

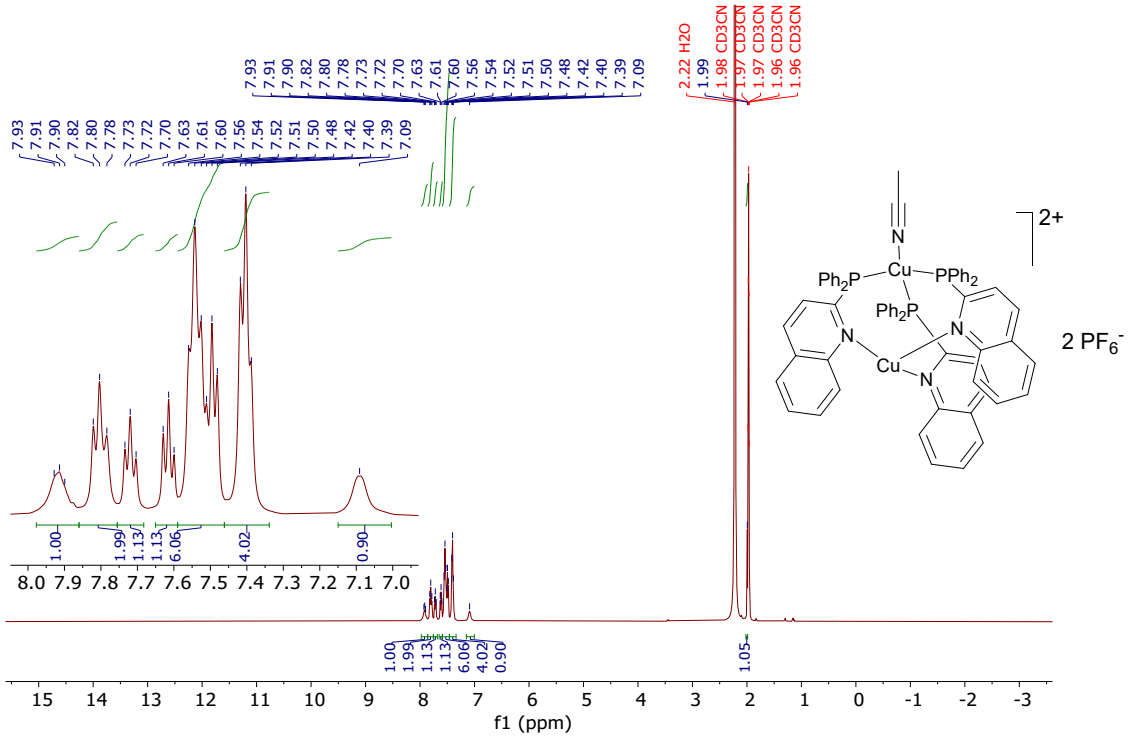

Figure S 29

^{13}C{^{1}H} NMR (126 MHz, CD_3CN)

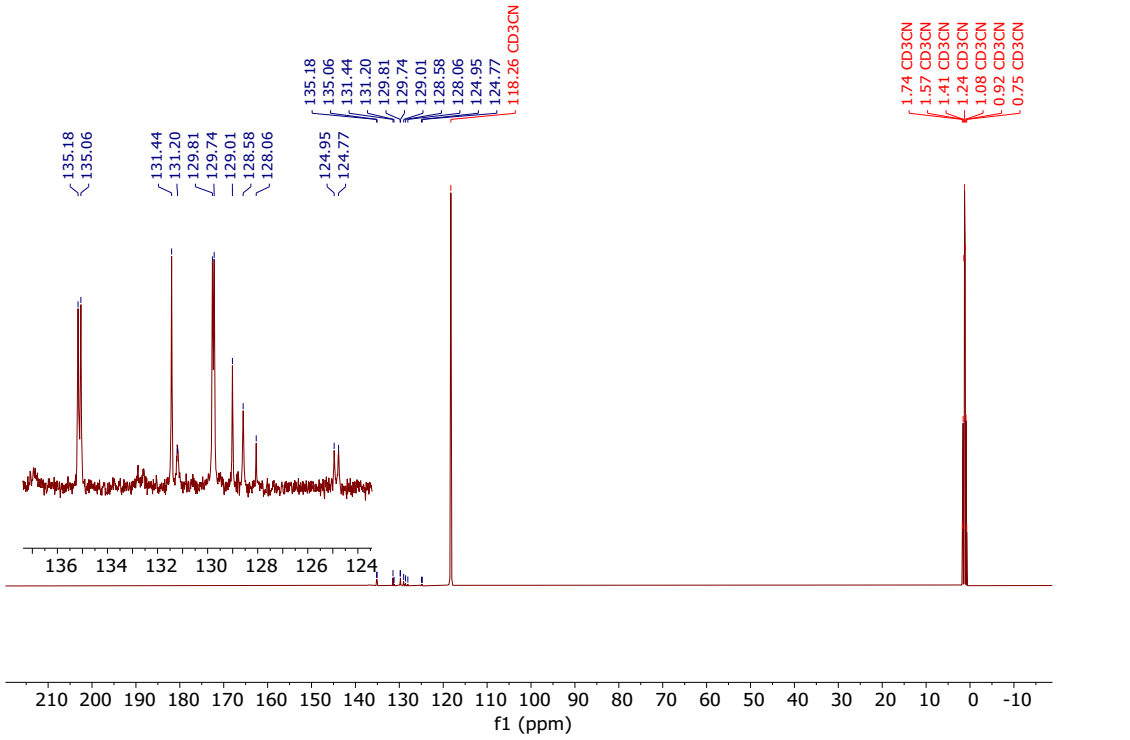

Figure S 30

$^{31}P\{^{1}H\}$ NMR (203 MHz, CD_3CN)

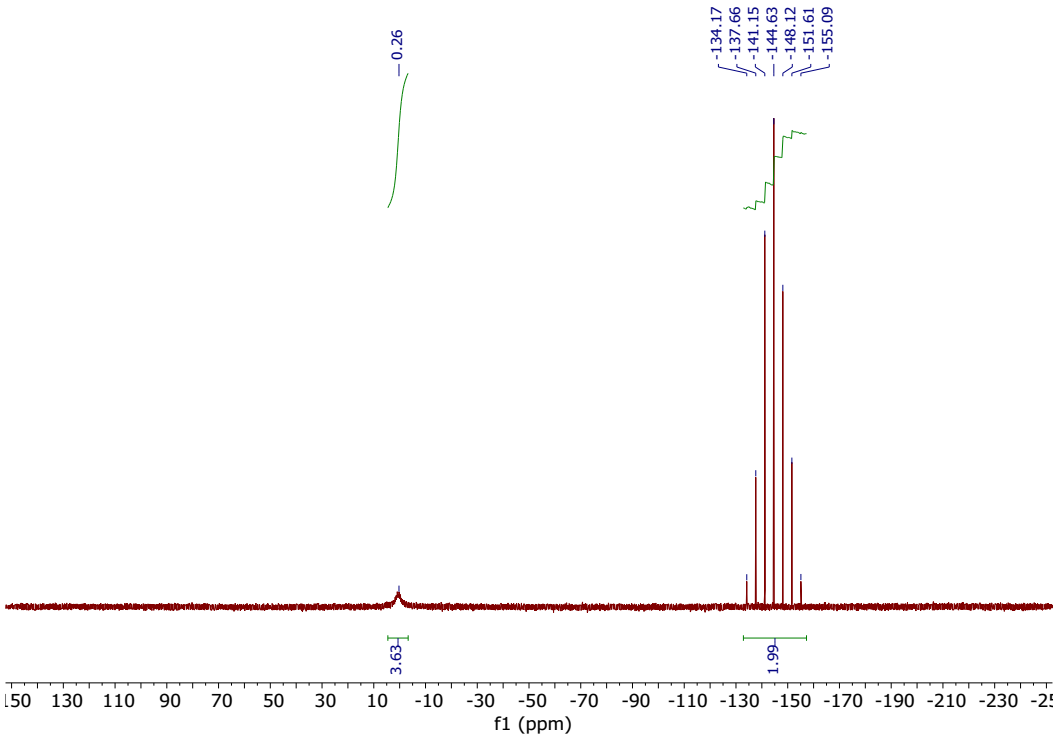

Figure S 31

2.5. 5-Cu-PF_6 after precipitation from reaction with Et_2O

^{1}H NMR (400 MHz, $CDCl_3$)

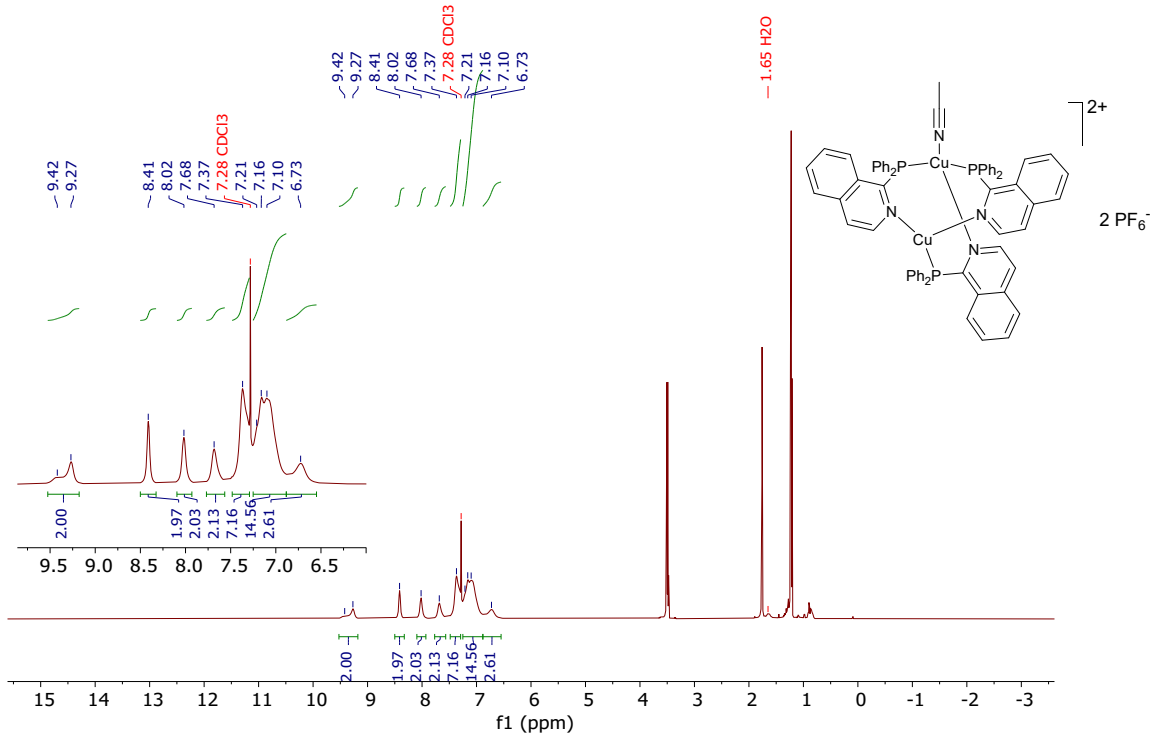

Figure S 32 Signals from residual Et_2O are visible on the spectrum. Residual Et_2O is visible in the spectrum. Shown HT structure is postulated based on crystal structure of **5-Cu-ClO_4** as well as the two ^{31}P signals at 14.6 and 7.8 ppm.

^{31}P{^{1}H,^{19}F} NMR (162 MHz, $CDCl_3$)

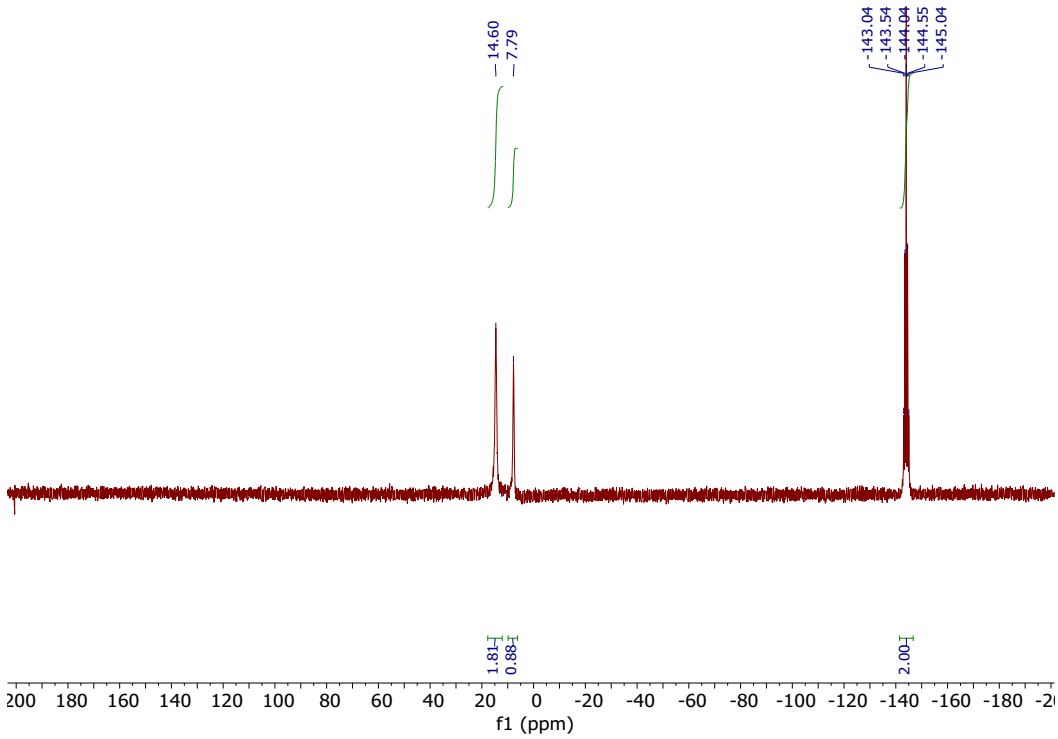

Figure S 33

^{19}F NMR (376 MHz, $CDCl_3$)

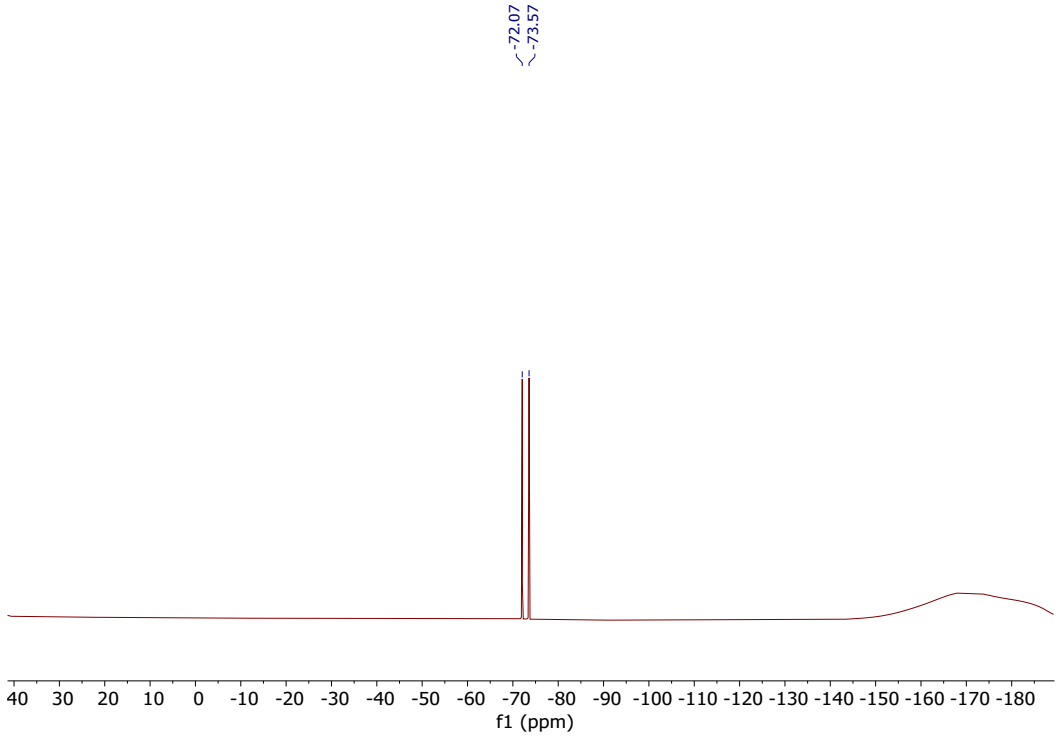

Figure S 34

2.6. 5-Cu-PF_6 dissolved in CD_3CN vs $CDCl_3$

^1H NMR (400 MHz)

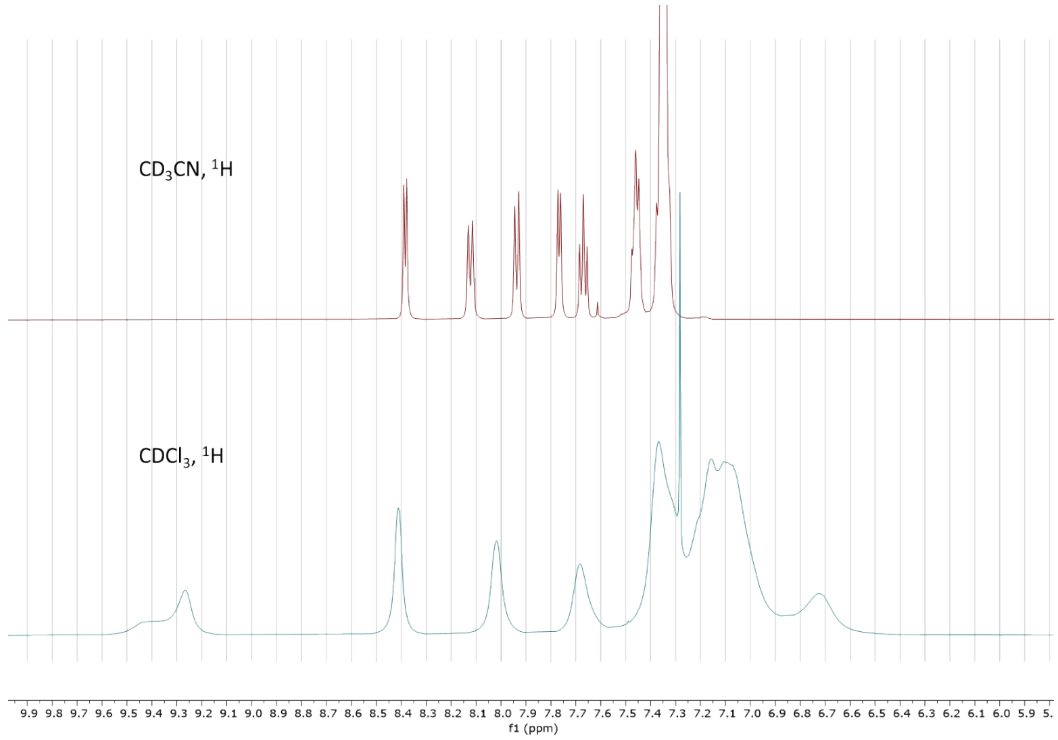

Figure S 35. ^1H NMR spectra of aromatic region of **5-Cu-PF_6** when dissolved in CD_3CN (top) and $CDCl_3$ (bottom).

^{31}P NMR (202 MHz)

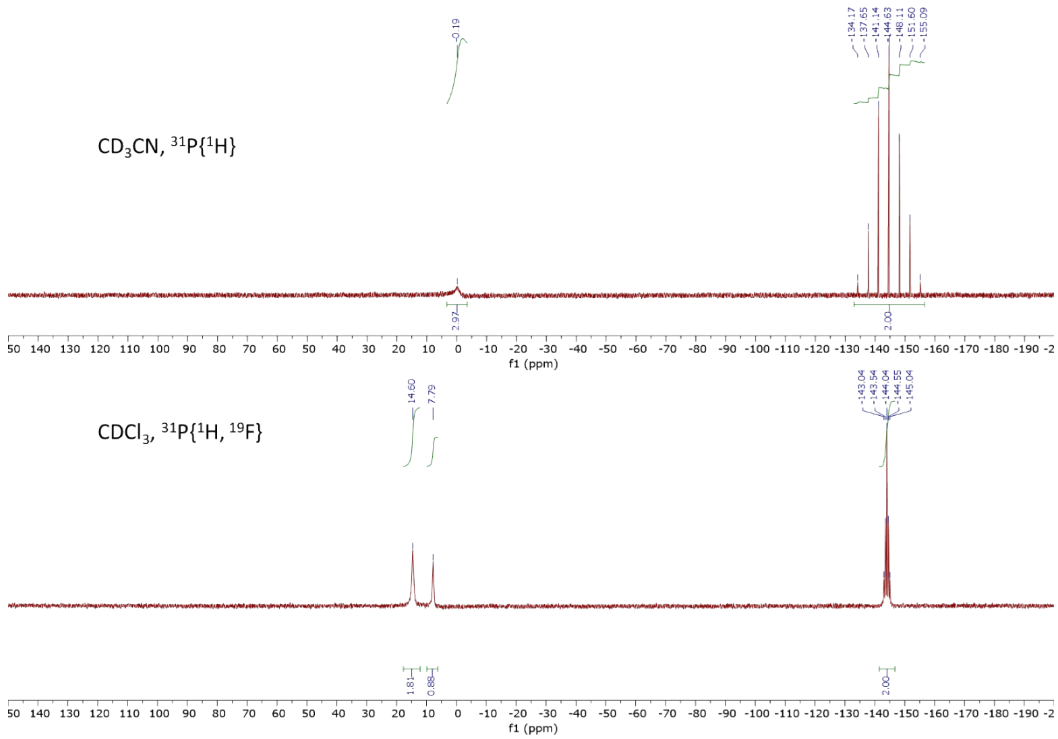

Figure S 36. ^{31}P NMR spectra of aromatic region of **5-Cu-PF$_6$** when dissolved in CD_3CN (top) and $CDCl_3$ (bottom).

2.7. 5-Cu-ClO_4^-

^{1}H NMR (500 MHz, $CDCl_3$)

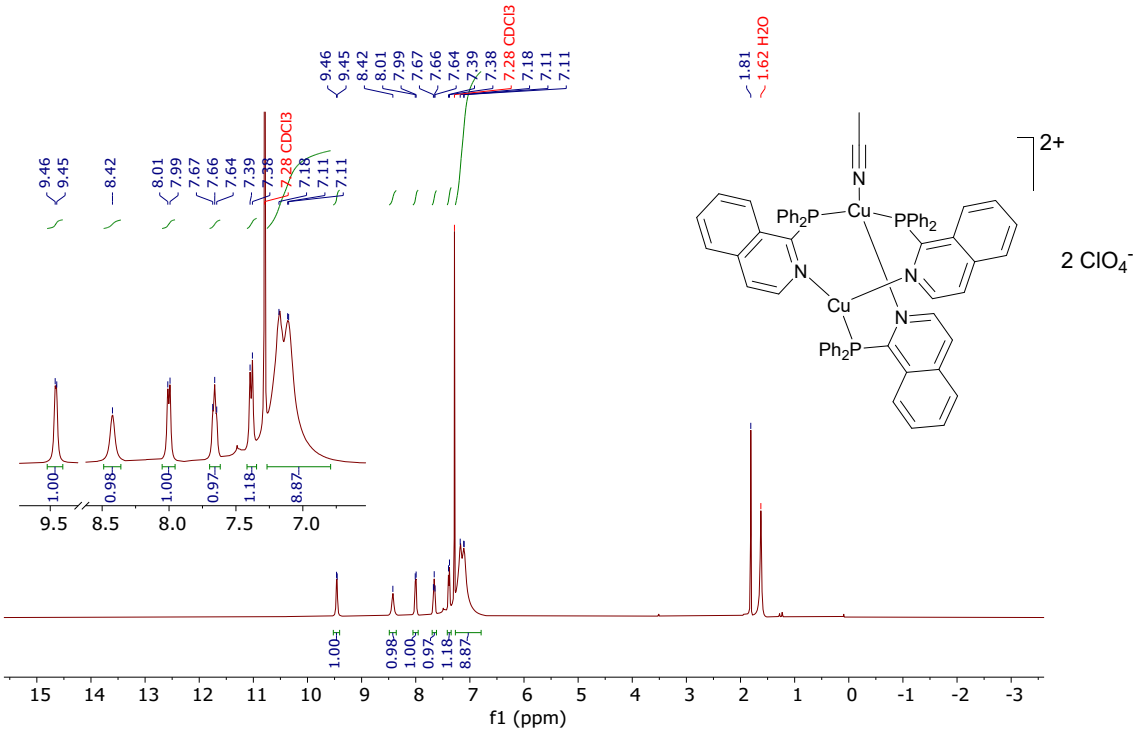

Figure S 37

^{31}P{^{1}H} NMR (202 MHz, $CDCl_3$)

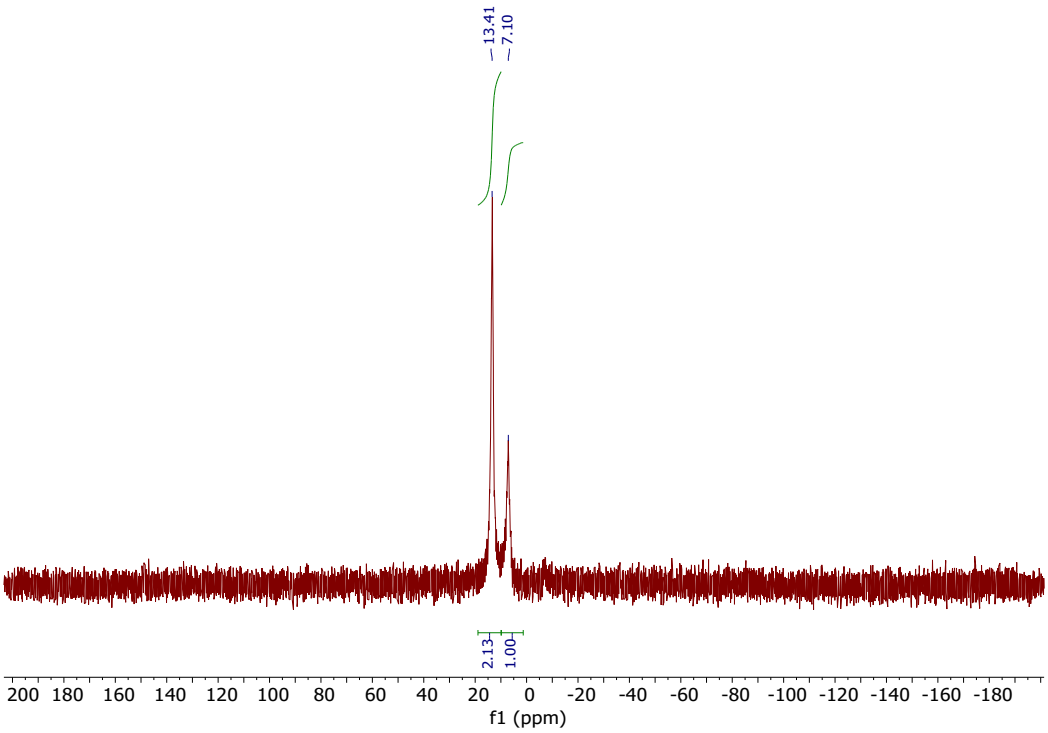

Figure S 38

2.8. 5-Cu-ClO_4^-, in the presence of NDMA

^{1}H NMR (500 MHz, $CDCl_3$)

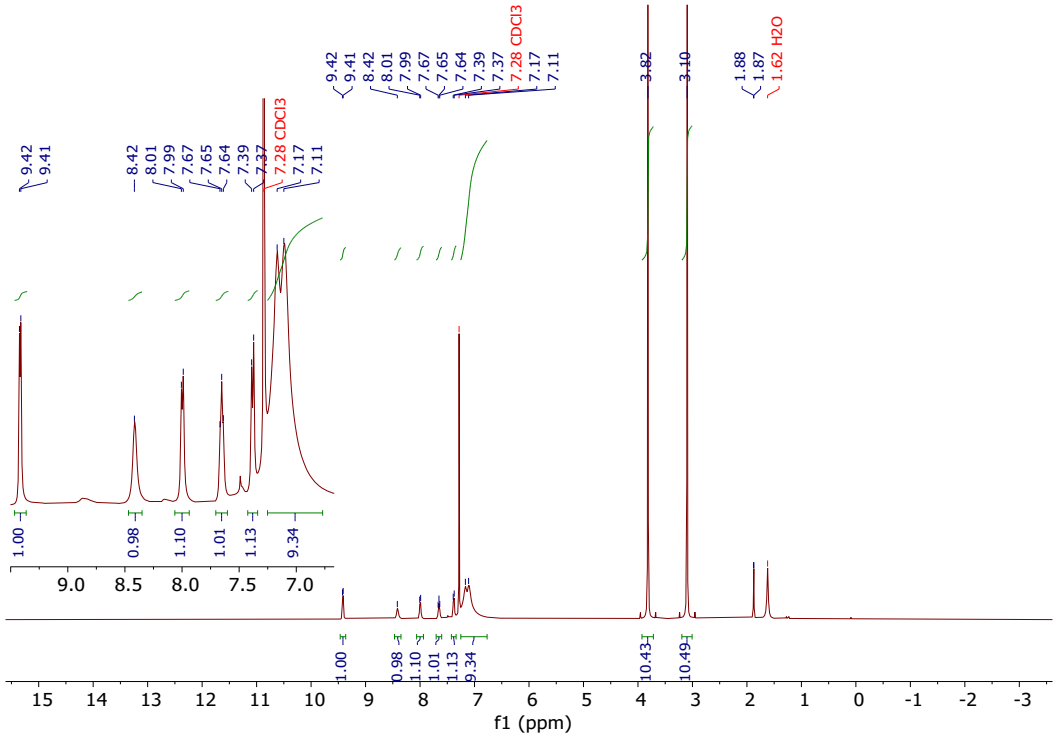

Figure S 39. NOTE: The two singlets at 3.8 and 3.1 ppm are from the two inequivalent methyl groups on NDMA due to restricted rotation about the N – N bond.

^{31}P{^{1}H} NMR (203 MHz, $CDCl_3$)

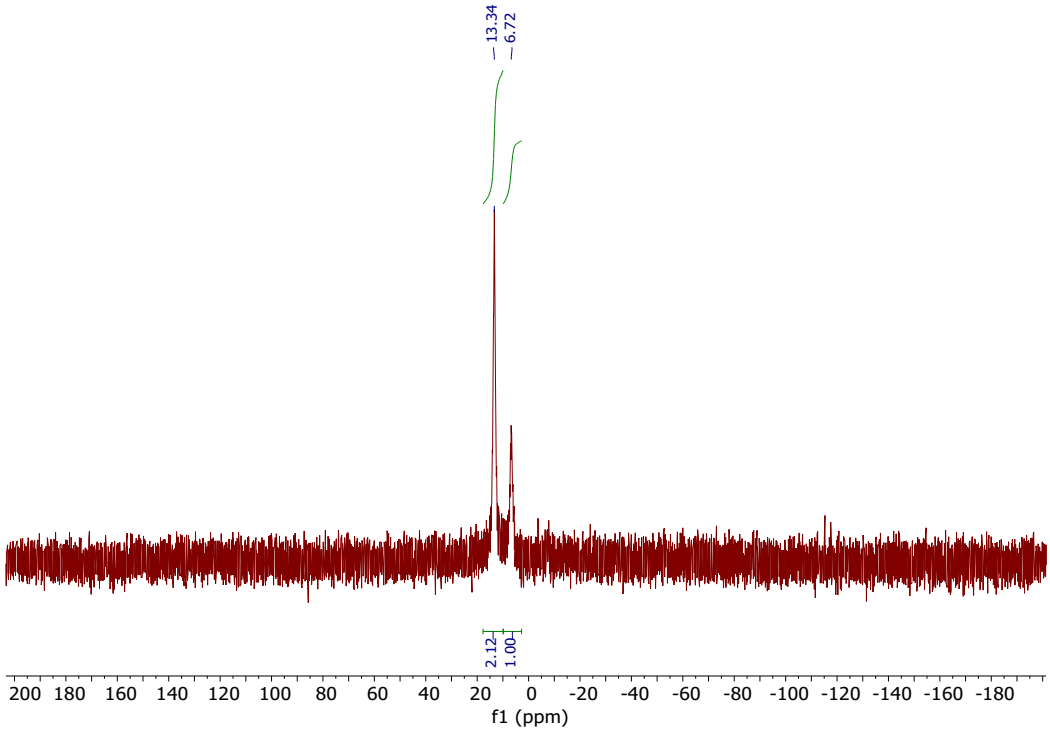

Figure S 40

2.9. Superimposed ^{1}H spectra of Figure S 37 and Figure S 39

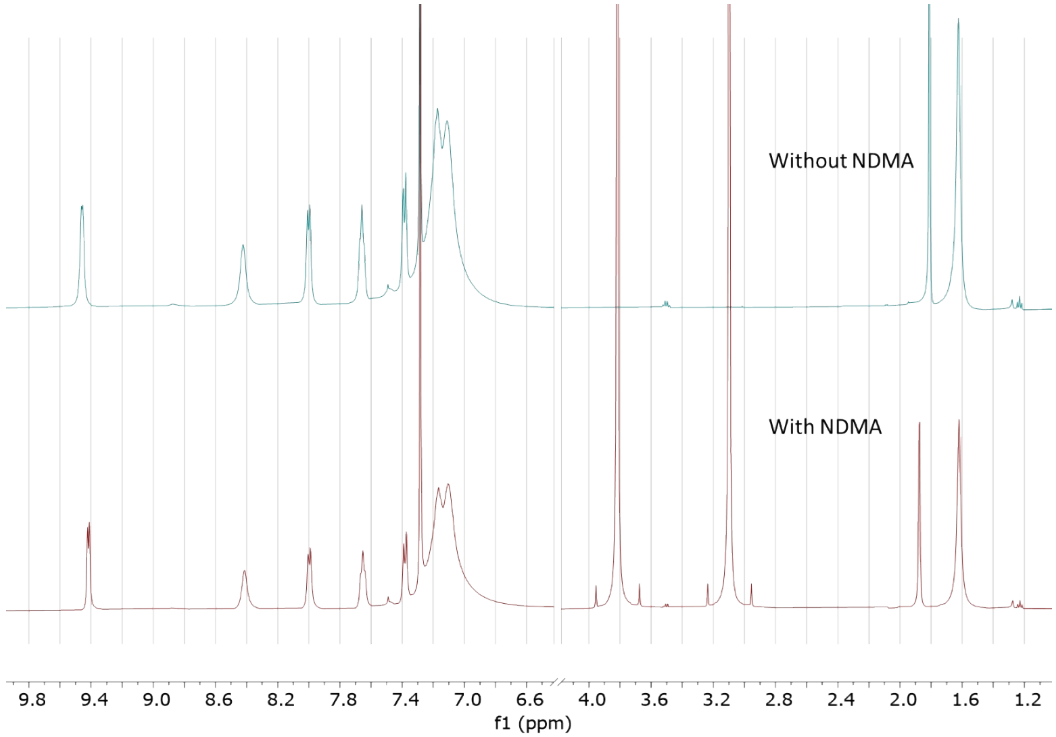

Figure S 41

2.10. Superimposed $^{31}P\{^{1}H\}$ spectra of Figure S 38 and Figure S 40

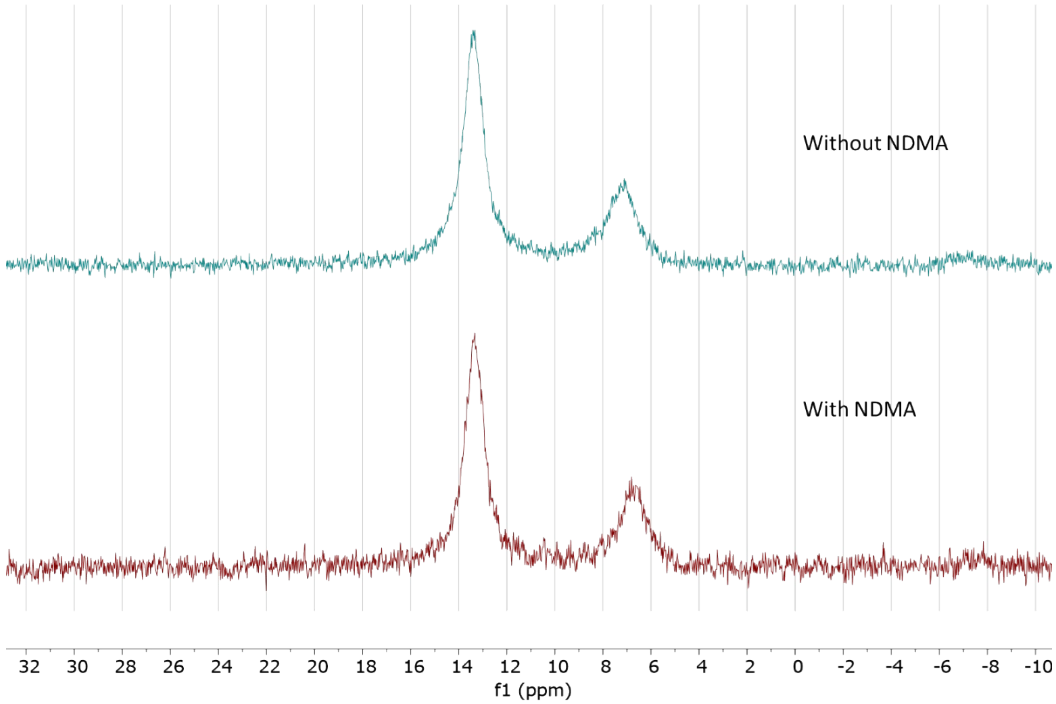

Figure S 42

2.11. 5-Cu-II from reacting 5 and $CuClO_4 \cdot 6H_2O$

^{1}H NMR (500 MHz, CD_3CN)

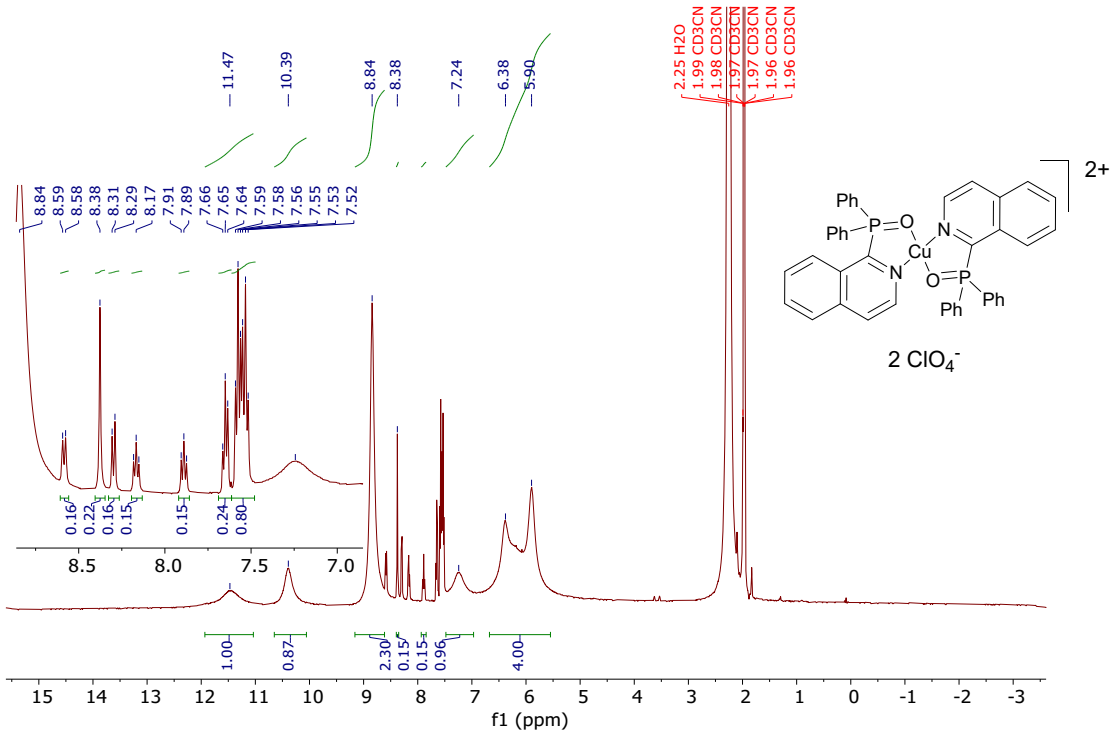

Figure S 43. The sharp signals are likely from intermediates during the oxidation process

^{31}P{^{1}H} NMR (202 MHz, CD_3CN)

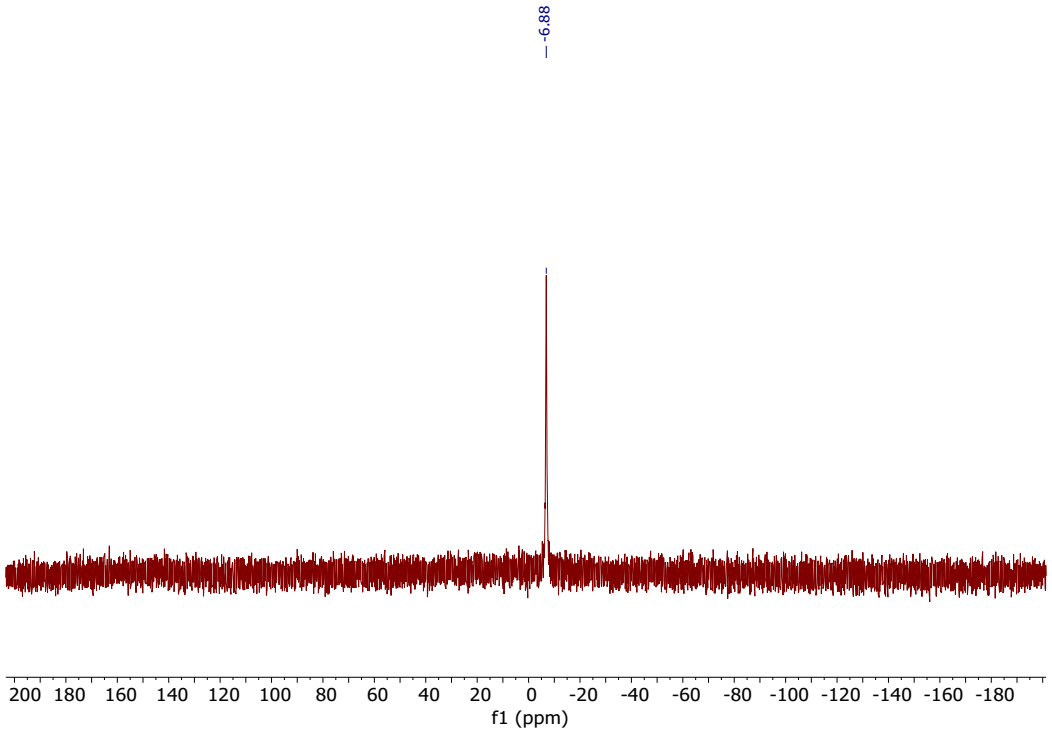

Figure S 44. This signal is likely from intermediates in the oxidation process

2.12. 5-Cu-II, with added NDMA

^{1}H NMR (500 MHz, CD_3CN)

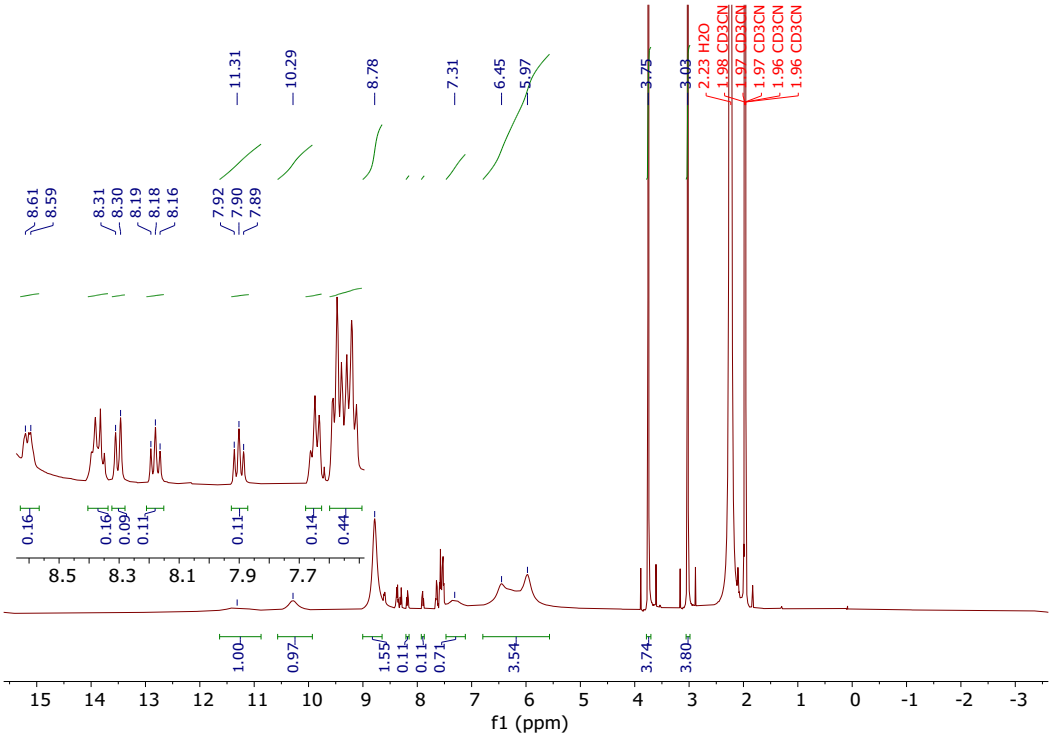

Figure S 45. NOTE: The two singlets at 3.8 and 3.1 ppm are from the two inequivalent methyl groups on NDMA due to restricted rotation about the N – N bond.

2.13. Superimposed ^{1}H spectra of Figure S 43 and Figure S 45

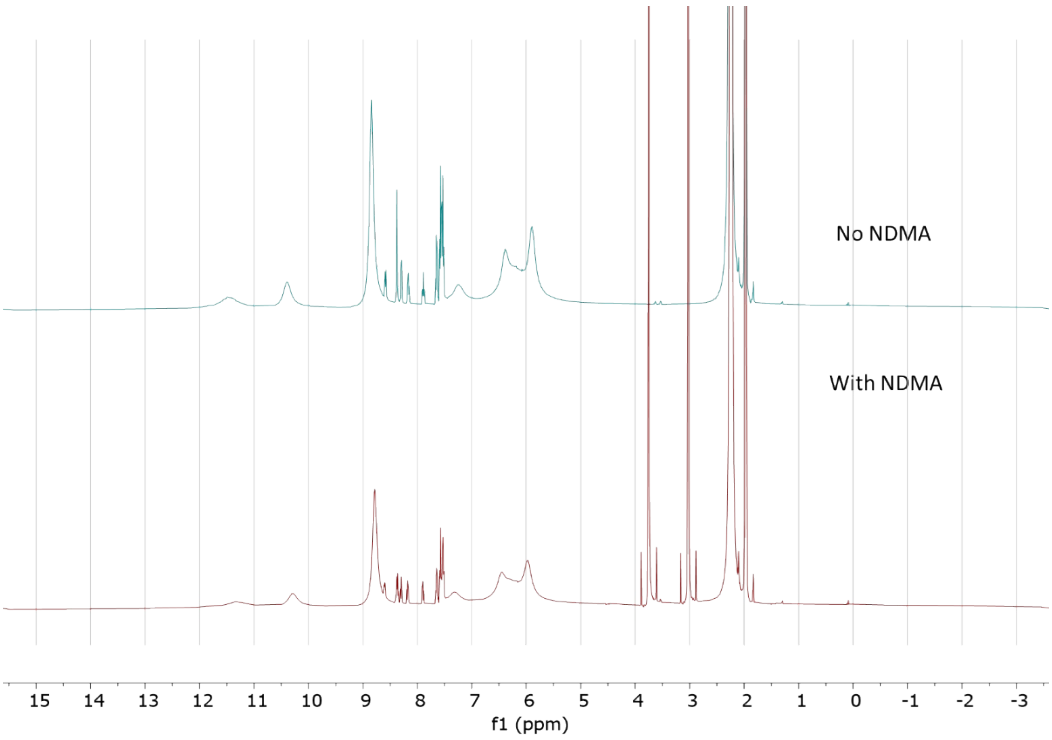

Figure S 46

2.14. Crude product of 5-Cu-II under different conditions in MeCN solution

^{1}H NMR (500 MHz, CD_3CN)

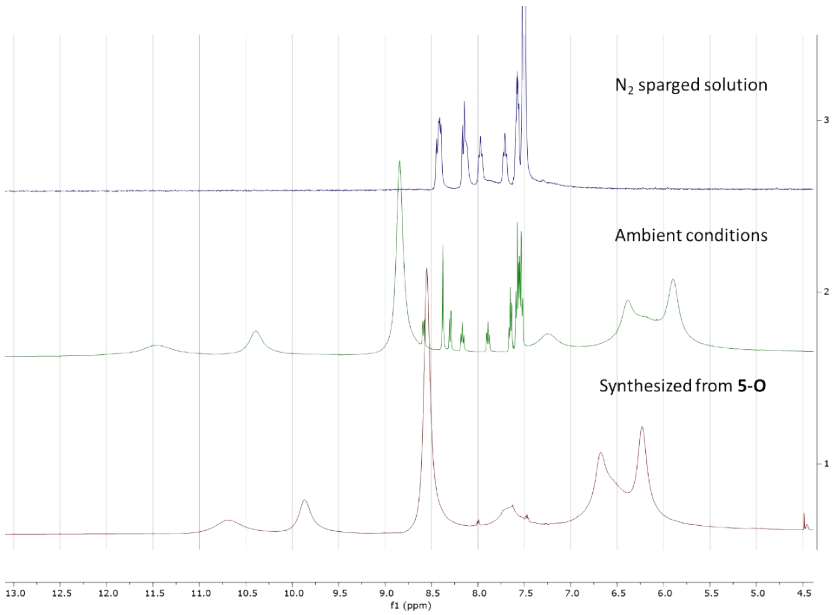

Figure S 47. Aromatic region of crude product after $CuClO_4{\cdot}6H_2O$ was added to a degassed solution of **5** (top); $CuClO_4{\cdot}6H_2O$ was added to an aerated solution of **5** (middle) and $CuClO_4{\cdot}6H_2O$ was added to an aerated solution of **5-O.** The broad signals attributable to **5-Cu-II** are not present in the absence of oxygen during synthesis.

^{31}P NMR (202 MHz, CD_3CN)

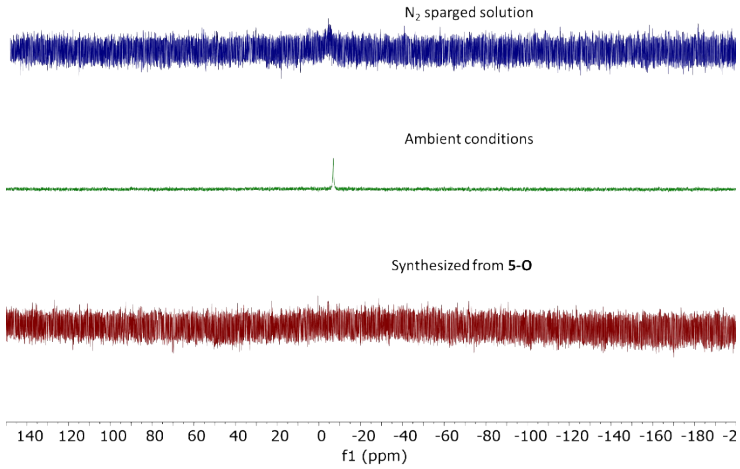

Figure S 48. ^{31}P NMR spectra of crude products from three different synthetic attempts towards **5-Cu-II**. $CuClO_4{\cdot}6H_2O$ was added to a degassed solution of **5** (top); $CuClO_4{\cdot}6H_2O$ was added to an aerated solution of **5** (middle) and $CuClO_4{\cdot}6H_2O$ was added to an aerated solution of **5-O.** The signal at –6.9 ppm is absent when starting from **5-O**, suggesting that it likely originates from intermediates during the oxidation process.

3. Experimental Details

$Cu(MeCN)_4PF_6$ may degrade over time and gain a blue coloration. It may be purified either by recrystallization from 1:1 MeCN:Et_2O or dissolving the mixture in MeCN and removing undissolved solids before removing the solvent to give a white powder. S_NAr reactions using 3-chloroisoquinoline, 2-chloroquinoline and 2-chloroquinazoline do not proceed favorably likely due to the LUMO of the aromatic system having larger coefficients at positions 1, 4, 5 and 8. An alternative synthetic strategy such as transition metal catalyzed coupling is recommended.

3.1. Crystallization conditions for X-ray diffraction

Single crystals of 1-Cu 1-Cu was dissolved in DCM and layered with MeOH. Single crystals were obtained via the slow evaporation of DCM.

Single crystals of 1-Cu-NDMA 1-Cu was dissolved in DCM and NDMA added. It was then layered with hexanes and crystals obtained upon mixing via diffusion.

Polycrystalline crystals of 2-Cu 2-Cu was dissolved in MeCN. Crystals were then grown from vapor diffusion with Et_2O at –20 °C.

Single crystals of 3-Cu 3-Cu was dissolved in DCM. Crystals were then grown from vapor diffusion with Et_2O.

Single crystals of 4-Cu 4-Cu was dissolved in MeCN and crystals grown from vapor diffusion with Et_2O.

Single crystals of 4-Cu-NDMA 4-Cu was dissolved in DCM and NDMA added. Crystals were then grown from vapor diffusion with Et_2O.

Single crystals of 5-Cu-ClO_4 5-Cu-ClO_4 was dissolved in $CHCl_3$, layered with toluene and left to stand. Single crystals were obtained upon mixing via diffusion.

Single crystals of 5-Cu-II 5-Cu-II was dissolved in MeCN. Crystals were then grown from vapor diffusion with Et_2O.

3.2. Preparation of samples for spectroscopic studies

Photoluminescent quantum yield spectra of 1-Cu and 1-Cu-NDMA The crystallized solids were separately added to a sample holder and placed in a Horiba Quanta-ϕ F-3029 integrating sphere. An excitation wavelength of 365 nm was used, the entry and exit slits were set to 0.6 and 0.8 nm respectively and the integration time was set to 0.5 s. A florescence spectrum was acquired with 1 nm increments from 345 to 720 nm to calculate quantum yields.

Solid state emission spectra of copper complexes 1-Cu, **2-Cu**, **3-Cu**, **5-Cu-PF_6** and **5-Cu-ClO_4** were each dissolved in $CHCl_3$. **4-Cu** and **5-Cu-II** were dissolved in MeCN. They were then dropcasted onto a quartz cover slip and the solvent removed in vacuo (15 min) before being mounted on a Horiba 1933 solid sample holder. 365 nm excitation was used, entry and exit slits were both set to 5 nm and the integration time was set to 0.1 s with an increment of 1 nm during sample data collection. The sample holder was rotated such that the excitation beam makes a anticlockwise angle of 30° to the normal of the sample holder surface. A background scan with only the sample holder and quartz coverslip was taken before sample data collection using an acquisition time of 1 s to be used for background subtraction. The main background signal comes from a scattering event, as changing the excitation wavelength results in a shift of the signal in the same direction.

3.3. Solution phase spectra

Emission Measurements: Before performing any sample measurements, a cuvette containing 3 ml of pure solvent ($CHCl_3$ or MeCN) is used to collect background signals with the primary signal being Raman scattering from residual water within the solvents. Entry and exit slits were set to 5 nm and integration time set to 1 s. Subsequently, this spectrum is subtracted from sample spectra to remove interfering signals. Acquired spectra were also corrected for emission response characteristics of the instrument which vary as a function of wavelength. The relevant correction file is termed “mcorrect” in the Fluorolog-3 operations manual. 365 nm excitation was used, entry and exit slits were both set to 5 nm and the integration time was set to 0.1 s with an increment of 1 nm during sample data collection. A GG400 bandpass filter was placed in front of the emission detector to eliminate the 2nd order diffraction signal at 730 nm.

The use of syringe filters is strongly discouraged due to introducing emissive contaminants when passing $CHCl_3$ or MeCN through the filter. If undissolved solids remain after sample preparation, the sample was left undisturbed to allow solids to settle out before carefully sampling the top of the solution for emission measurements. Alternatively for denser solvents like $CHCl_3$, the sample may be transferred to polypropylene centrifuge tubes and centrifuged to sample the supernatant. If a syringe filter is used a background acquisition should be performed using the filtered solvent to deconvolute interfering signals.

Excitation Measurements: A background scan is first performed using a quartz cuvette containing pure solvent with an integration time of 1s with both entrance and exit slits set to 5 nm. The sample is then introduced and the emission detector set to the wavelength with highest emission intensity. The background was subtracted post data acquisition. A GG400 bandpass filter was placed in front of the emission detector and a UG1 bandpass filter was placed in front of the excitation beam.

3.3.1. Complexes

1-Cu 1.4 mg of material was diluted to 10 ml in $CHCl_3$ in a volumetric flask to give solution **A** (150 µM). NDBA (1 µl) was diluted with solution **A** (125 µl) to give a stock solution of NDBA (solution **B**). The emission spectrum of solution **A1** (3 ml of solution **A**) was acquired using 365 nm excitation. The spectrum was acquired a total of 2 times to ensure consistency, waiting (at least 10 s) after the first acquisition ends before starting the second. To introduce 0.2, 1, 5 and 12 equivalents of NDBA to solution **A1**: 2, 8, 40 and 70 µl of solution **B** were added to the same sample of solution **A1**. After each NDBA addition, emission spectra were acquired until 2 consistent sets of data were obtained, waiting 10 s before starting a subsequent acquisition.

For absorption measurements, solution **A** (250 µl) was diluted to 3 ml before data acquisition.

2-Cu 2.1 mg was diluted to 10 ml in a volumetric flask using $CHCl_3$ to give solution **A** (150 µM). NDBA (1 µl) was diluted by solution **A** (125 µl) to give solution **B**. Measurements were conducted following the steps outlined for **1-Cu.**

3-Cu (M_w = 1398) 2.1 mg was diluted to 10 ml in a volumetric flask using $CHCl_3$ to give solution **A** (150 µM). NDBA (1 µl) was diluted by solution **A** (125 µl) to give solution **B**. To introduce 0.2, 0.4, 0.6, 0.8, 1 equivalent of NDBA to solution **A1**: 2 µl of solution **B** were sequentially added to the same sample of solution **A1**. 10 µl of solution **B** was then added to introduce a total of 2 equivalents of NDBA, followed by sequential adding of 20 µl of solution **B** to get 4, 6, 8, 10 and 12 equivalents of NDBA. After each NDBA addition, emission spectra were acquired until 2 consistent sets of data were obtained, waiting 10 s before starting a subsequent acquisition.

4-Cu 2.1 mg was diluted to 10 ml in a volumetric flask using MeCN to give solution **A** (150 µM). NDBA (1 µl)/ DBA (1 µl) was diluted by solution **A** (125 µl/ 125 µl) to give solution **B**. Measurements were conducted following the steps outlined for **1-Cu.**

5-Cu-PF_6 2.1 mg was diluted to 10 ml in a volumetric flask using $CHCl_3$ to give solution **A** (150 µM). NDBA (1 µl)/ NDMA (1 µl)/ DBA (1 µl) was diluted by solution **A** (125 µl/ 300 µl / 125 µl) to give solution **B**. Measurements were conducted following the steps outlined for **1-Cu.**

5-Cu-ClO_4 2.05 mg was diluted to 10 ml in a volumetric flask with either $CHCl_3$ or MeCN to give solution **A** (150 µM). NDBA (1 µl) was diluted with solution **A** (125 µl) to give solution **B**. Measurements were conducted following the steps outlined for **1-Cu.**

5-Cu-II 1.47 mg was diluted to 10 ml in a volumetric flask with MeCN to give solution **A** (150 µM). NDBA (1 µl) was diluted with solution **A** (125 µl) to give solution **B**. Measurements were conducted following the steps outlined for **1-Cu.** For excitation measurements, the detector was set to 420 nm.

3.3.2. Phosphines

Phosphine concentrations were set at 450 µM as each binuclear complex contains three P^N ligands.

1 1.2 mg was diluted to 10 ml in a volumetric flask with $CHCl_3$ to give solution **A** for emission measurements (450 µM) as each molecule of the complex contains 3 times the amount of phosphine. For absorption measurements, solution **A** (250 µl) was diluted to 3 ml before data acquisition.

2 1.4 mg was diluted to 10 ml in a volumetric flask with $CHCl_3$ to give solution **A** for emission measurements (450 µM). For absorption measurements, solution **A** (250 µl) was diluted to 3 ml before data acquisition.

3 1.4 mg was diluted to 10 ml in a volumetric flask with $CHCl_3$ to give solution **A** for emission measurements (450 µM). For absorption measurements, solution **A** (250 µl) was diluted to 3 ml before data acquisition.

4 1.4 mg was diluted to 10 ml in a volumetric flask with MeCN to give solution **A** for emission measurements (450 µM). For absorption measurements, solution **A** (250 µl) was diluted to 3 ml before data acquisition.

5 1.4 mg was diluted to 10 ml in a volumetric flask with $CHCl_3$ to give solution **A** for emission measurements (450 µM). For absorption measurements, solution **A** (250 µl) was diluted to 3 ml before data acquisition.

5-O 1.4 mg was diluted to 10 ml in a volumetric flask with either $CHCl_3$ or MeCN to give solution **A** for emission measurements (450 µM). For absorption measurements, solution **A** (250 µl) was diluted to 3 ml before data acquisition. For excitation measurements the detector was set to 420 nm.

PPh_3 1.2 mg was diluted to 10 ml in a volumetric flask with $CHCl_3$ to give solution **A** for emission measurements (450 µM). For absorption measurements, solution **A** (250 µl) was diluted to 3 ml before data acquisition.

3.4. Stern-Volmer analysis

The Stern-Vomer equation may be expressed as

$$F_0/F = 1 + K_{SV}[Q]$$, where

F_0 = Fluorescence intensity with no quencher (blank)

F = Fluorescence intensity in the presence of quencher at different concentrations

K_{SV} = Stern-Volmer constant

[Q] = Concentration of quencher (NDMA/ NDBA/ DBA)

The wavelength chosen for analysis corresponds to that with the highest emission intensity in the absence of quencher for each Cu complex examined. The corrected intensity values were extracted and normalized to give F_0/F values. Plotting F_0/F against [Q] and fitting of the data where emission changes were linear with respect to quencher equivalents gives a value for K_{SV}. At least two scans of the same sample were performed for each concentration of quencher to order to obtain intensity (**x̄**) and standard deviation (**s**) values.

3.4.1. Limit of detection calculation example

The formula used for calculating the limit of detection (L.O.D) is adapted from literature,[1] where the recommendation was to define it as three times the standard deviation value of a blank sample on a calibration plot. In the Stern-Volmer analysis, **s**(F_0/F) was computed as

$$s\left({}^{F_0}\!/_{F}\right) = \frac{s(F)}{\bar{x}(F)}$$

in order to keep the proportion constant relative to the raw intensity data. For the titration measurement on **3-Cu**, the blank sample had

$$\bar{x} = 229626 \text{ and } s = 6286 \text{ which gives}$$

$$s\left({}^{F_0}\!/_{F}\right) = 0.02737$$

This gives a limit of detection value for $F_0/F = 1 - 3 \times 0.02737 = 0.9179$, which corresponds to [Q] = 0.12 equivalents of NDMA. **[3-Cu]** during the measurements was 150 µM, which translates to [NDBA] = 18 µM = 2.8 ppm at the detection limit, given that M_w of NDBA is 158.

4. Crystallographic data

Table S 1 Crystal refinement parameters on reported complexes

Crystal data	1-Cu (CCDC 2218761)	3-Cu (CCDC 2218766)	4-Cu (CCDC 2218759)
Chemical formula	$C_{49}H_{42}Cu_2N_6OP_3$·2(F_6P)·1.303(CH_3O)	$C_{67}H_{53}Cl_6Cu_2F_{12}N_4P_5$	$C_{65}H_{51}Cu_2F_{12}N_4P_5$
M_r	1281.23	1636.76	1398.02
Crystal system, space group	Monoclinic, $P2_1/n$	Monoclinic, $P2_1/c$	Monoclinic, $P2_1/n$
Temperature (K)	100	100	100
a, b, c (Å)	12.4787 (2), 21.7573 (4), 19.9382 (4)	12.4808 (10), 23.632 (2), 23.161 (2)	16.2335 (12), 15.8978 (11), 22.7583 (15)
β (°)	90.6313 (8)	97.416 (3)	90.055 (3)
V (Å³)	5412.95 (17)	6774.3 (10)	5873.4 (7)
Z	4	4	4
Radiation type	Mo *K*α	Mo *K*α	Mo *K*α
μ (mm⁻¹)	1.02	1.06	0.95
Crystal size (mm)	0.35 × 0.27 × 0.17	0.31 × 0.17 × 0.15	0.18 × 0.14 × 0.04
Data collection			
Diffractometer	Bruker Photon3 CPAD	Bruker Photon3 CPAD	Bruker Photon3 CPAD
Absorption correction	Multi-scan SADABS (Herbst-Irmer et al., 2015)	Multi-scan SADABS (Herbst-Irmer et al., 2015)	Multi-scan SADABS (Herbst-Irmer et al., 2015)
T_{min}, T_{max}	0.546, 0.605	0.567, 0.640	0.688, 0.746
No. of measured, independent and observed [$I > 2\sigma(I)$] reflections	254045, 18027, 15809	645915, 25821, 21461	210392, 19561, 15180
R_{int}	0.044	0.055	0.052
$(\sin \theta/\lambda)_{max}$ (Å⁻¹)	0.735	0.769	0.735
Refinement			
$R[F^2 > 2\sigma(F^2)]$, $wR(F^2)$, S	0.032, 0.081, 1.08	0.041, 0.115, 1.04	0.044, 0.115, 1.04
No. of reflections	18027	25821	19561
No. of parameters	918	1596	858
No. of restraints	3145	6241	1173
H-atom treatment	H-atom parameters constrained	H-atom parameters constrained	H-atom parameters constrained
$\Delta\rho_{max}$, $\Delta\rho_{min}$ (e Å⁻³)	0.74, −0.56	1.00, −1.04	0.61, −1.28

Table S 1 (continued)

Crystal data	5-Cu-ClO4 (CCDC 2218763)	1-Cu-NDMA (CCDC 2218762)	4-Cu-NDMA (CCDC 2218765)
Chemical formula	$C_{65}H_{51}Cu_2N_4P_3{\cdot}2(C_7H_8){\cdot}2(ClO_4){\cdot}CHCl_3$	$C_{50}H_{45}Cu_2F_{12}N_8OP_5$	$0.79(C_{65}H_{51}Cu_2N_4P_3){\cdot}0.21(C_{65}H_{54}Cu_2N_5OP_3){\cdot}2(F_6P)$
M_r	1610.62	1283.87	1404.96
Crystal system, space group	Monoclinic, $P2_1/n$	Monoclinic, $P2_1/n$	Monoclinic, $P2_1/n$
Temperature (K)	100	100	100
a, b, c (Å)	13.1266 (8), 43.931 (3), 13.5378 (9)	12.3403 (4), 21.7180 (7), 19.9719 (6)	16.304 (2), 15.872 (2), 22.919 (3)
β (°)	106.065 (2)	91.9247 (12)	90.583 (5)
V (Å³)	7501.9 (8)	5349.6 (3)	5930.3 (14)
Z	4	4	4
Radiation type	Mo *K*α	Mo *K*α	Mo *K*α
μ (mm⁻¹)	0.87	1.03	0.94
Crystal size (mm)	0.16 × 0.16 × 0.05	0.25 × 0.23 × 0.17	0.14 × 0.14 × 0.03
Data collection			
Diffractometer	Bruker Photon3 CPAD	Bruker Photon3 CPAD	Bruker Photon3 CPAD
Absorption correction	Multi-scan SADABS (Herbst-Irmer et al., 2015)	Multi-scan SADABS (Herbst-Irmer et al., 2015)	Multi-scan SADABS (Herbst-Irmer et al., 2015)
T_{min}, T_{max}	0.668, 0.746	0.611, 0.660	0.681, 0.725
No. of measured, independent and observed [$I > 2\sigma(I)$] reflections	289237, 24979, 21457	268078, 16323, 14477	478033, 20655, 17187
R_{int}	0.055	0.091	0.054
$(\sin\theta/\lambda)_{max}$ (Å⁻¹)	0.735	0.714	0.746
Refinement			
$R[F^2 > 2\sigma(F^2)]$, $wR(F^2)$, S	0.049, 0.102, 1.20	0.066, 0.182, 1.09	0.038, 0.097, 1.04
No. of reflections	24979	16323	20655
No. of parameters	922	882	1026
No. of restraints		1444	3573
H-atom treatment	H-atom parameters constrained	H-atom parameters constrained	H-atom parameters constrained
	$w = 1/[\sigma^2(F_o^2) + (0.0072P)^2 + 14.015P]$ where $P = (F_o^2 + 2F_c^2)/3$	$w = 1/[\sigma^2(F_o^2) + (0.0375P)^2 + 45.6337P]$ where $P = (F_o^2 + 2F_c^2)/3$	
$\Delta\rho_{max}$, $\Delta\rho_{min}$ (e Å⁻³)	0.97, −0.69	0.78, −0.73	0.48, −0.97

Table S 1 (continued)

Crystal data	5-Cu-II (CCDC 2218764)	5-Cu-II-NDMA (CCDC 2218758)	5-Cu-NDMA (CCDC 2218757)
Chemical formula	$C_{42}H_{32}Cl_2CuN_2O_{10}P_2$	$C_{42}H_{32}Cl_2CuN_2O_{10}P_2$	$C_{63}H_{48}ClCu_2N_3O_4P_3{\cdot}ClO_4{\cdot}1.5(C_7H_8)$
M_r	921.07	921.07	1404.13
Crystal system, space group	Orthorhombic, *Pbca*	Triclinic, *P*	Triclinic, *P*
Temperature (K)	100	100	100
a, b, c (Å)	14.8421 (12), 22.3318 (16), 23.2202 (18)	10.9585 (5), 14.9847 (7), 19.6805 (10)	13.4113 (5), 22.0711 (8), 22.7575 (8)
α, β, γ (°)		83.8641 (14), 78.2297 (14), 88.8782 (14)	97.767 (3), 90.925 (3), 103.689 (3)
V (Å^3)	7696.4 (10)	3145.6 (3)	6476.8 (4)
Z	8	3	4
Radiation type	Mo *K*α	Mo *K*α	Cu *K*α
μ (mm^{-1})	0.86	0.78	2.76
Crystal size (mm)	0.26 × 0.13 × 0.04	0.19 × 0.14 × 0.03	0.13 × 0.05 × 0.01
Data collection			
Diffractometer	Bruker Photon3 CPAD	Bruker Smart *APEX2* CCD	Bruker Photon3 CPAD
Absorption correction	Multi-scan SADABS (Herbst-Irmer et al., 2015)	Multi-scan SADABS (Herbst-Irmer et al., 2015)	Multi-scan SADABS (Herbst-Irmer et al., 2015)
T_{min}, T_{max}	0.618, 0.695	0.659, 0.695	0.534, 0.621
No. of measured, independent and observed [$I > 2\sigma(I)$] reflections	305955, 12818, 10704	178169, 18393, 13453	22338, 22338, 14753
R_{int}	0.065	0.052	0.096
$(\sin\theta/\lambda)_{max}$ (Å^{-1})	0.735	0.704	0.604
Refinement			
$R[F^2 > 2\sigma(F^2)]$, $wR(F^2)$, S	0.042, 0.106, 1.09	0.043, 0.113, 1.02	0.079, 0.180, 1.07
No. of reflections	12818	18393	22338
No. of parameters	532	1251	1760
No. of restraints		3067	3186
H-atom treatment	H-atom parameters constrained	H-atom parameters constrained	H-atom parameters constrained
			$w = 1/[\sigma^2(F_o^2) + (0.0477P)^2 + 34.8098P]$ where $P = (F_o^2 + 2F_c^2)/3$
$\Delta\rho_{max}$, $\Delta\rho_{min}$ (e Å^{-3})	0.78, −0.76	0.52, −0.61	0.69, −0.82

Table S 1 (continued)

Crystal data	3-Cu-NDMA (CCDC 2218760)
Chemical formula	$C_{73}H_{71}Cu_2F_{12}N_4O_2P_5$
M_r	1546.26
Crystal system, space group	Monoclinic, $P2_1/c$
Temperature (K)	100
a, b, c (Å)	24.7829 (8), 14.8540 (5), 19.2868 (6)
α, β, γ (°)	101.6928 (19)
V (Å^3)	6952.6 (4)
Z	4
Radiation type	Cu *K*α
μ (mm^{-1})	2.54
Crystal size (mm)	0.36 × 0.12 × 0.06
Data collection	
Diffractometer	Bruker Photon3 CPAD
Absorption correction	Multi-scan
	SADABS (Herbst-Irmer et al., 2015)
T_{min}, T_{max}	0.198, 0.355
No. of measured, independent and	258032, 12764, 11654
observed [$I > 2\sigma(I)$] reflections	
R_{int}	0.057
$(\sin \theta/\lambda)_{max}$ (Å^{-1})	0.603
Refinement	
$R[F^2 > 2\sigma(F^2)]$, $wR(F^2)$, S	0.081, 0.219, 1.11
No. of reflections	12764
No. of parameters	1097
No. of restraints	3429
H-atom treatment	H-atom parameters constrained
	$w = 1/[\sigma^2(F_o^2) + (0.0823P)^2 + 27.6755P]$
	where $P = (F_o^2 + 2F_c^2)/3$
$\Delta\rho_{max}$, $\Delta\rho_{min}$ (e Å^{-3})	1.03, −0.60

5. Crystal structures and selected measurements

5.1. 1-Cu

Selected distances

Atoms	Distance (Å)
Cu1–P1	2.2529(4)
Cu1–P2	2.2126(5)
Cu1–N5	2.0021(9)
Cu2–N1	2.0794(9)
Cu2–N2	2.1327(9)
Cu2–P3	2.2406(6)
Cu2–O1T	2.1894(18)
Cu1–Cu2	2.6262(6)

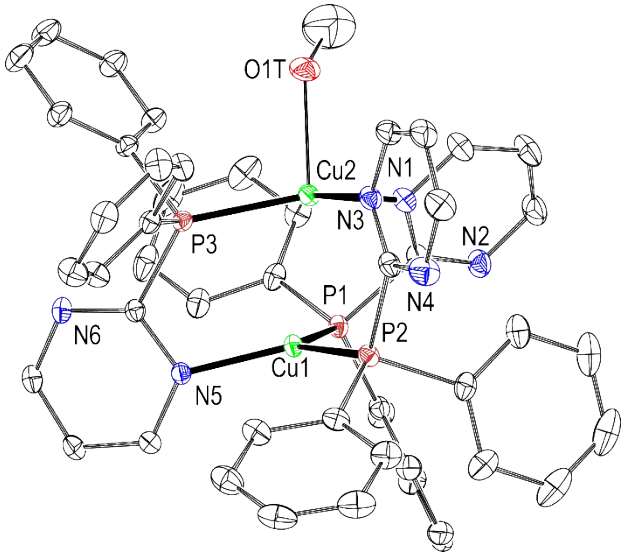

Figure S 49

5.2. 3-Cu major linkage isomer

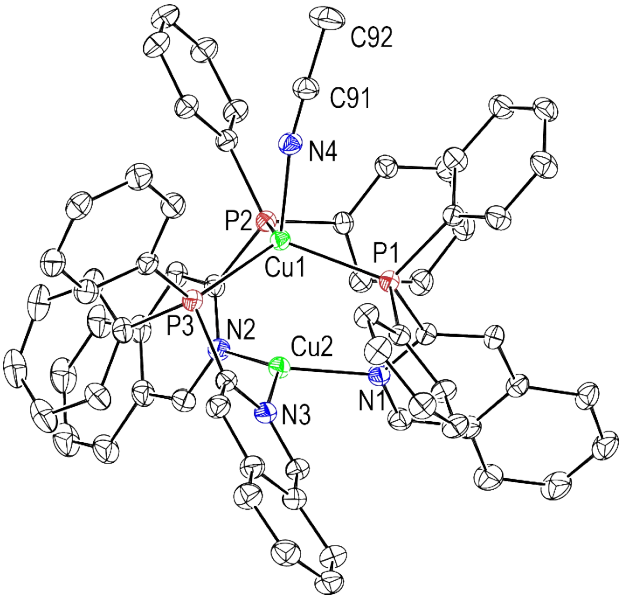

Selected distances / Selected angles

Atoms	Distance (Å)	Atoms	Bond Angle (°)
Cu1–N4	2.0256(17)	Cu1–N4 – C91	165.89(16)
N4–C91	1.142(3)	N4–C91–C92	178.5(2)
Cu1–P1	2.3465(11)		
Cu1–P2	2.3366(11)		
Cu1–P3	2.3392(6)		
Cu2–N1	2.0142(19)		
Cu2–N2	1.961(3)		
Cu2–N3	1.9869(15)		
Cu1–Cu2	2.7125(6)		

Figure S 50

5.3. 3-Cu minor linkage isomer

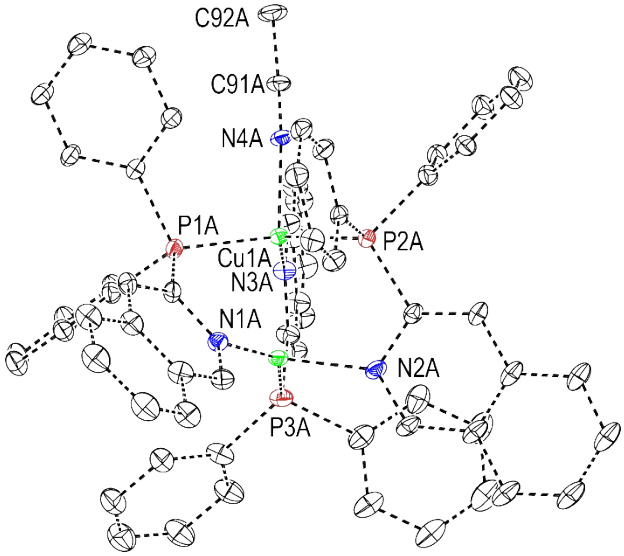

Selected distances

Selected angles

Atoms	Distance (Å)	Atoms	Bond Angle (°)
Cu1A–N4A	2.059(13)	Cu1A–N4 A–C91A	176.1(19)
N4A–C91A	1.135(19)	N4A–C91A–C92A	176(3)
Cu1A–P1A	2.318(13)		
Cu1A–P2A	2.307(13)		
Cu1A–N3A	2.114(11)		
Cu2A–N1A	2.024(18)		
Cu2–N2	2.10(4)		
Cu2A–P3A	2.223(7)		
Cu1–Cu2	2.654(5)		

Figure S 51

5.4. 4-Cu

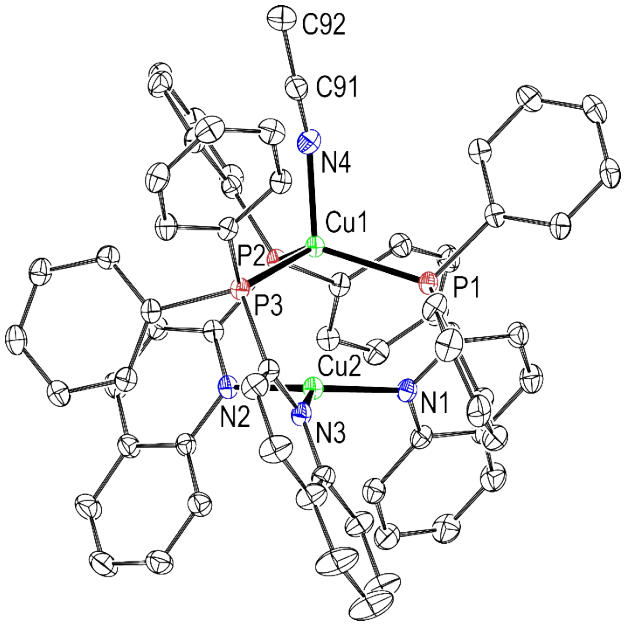

Figure S 52

Selected distance

Selected angles

Atoms	Distance (Å)	Atoms	Bond Angle (°)
Cu1–N4	2.0403(18)	Cu1–N4 –C91	166.02(17)
N4–C91	1.132(3)	N4–C91–C92	178.3(2)
P1–Cu1	2.3125(7)		
P2–Cu1	2.3141(6)		
P3–Cu1	2.3127(6)		
N1–Cu2	2.0243(17)		
N2–Cu2	2.0414(16)		
N3–Cu2	2.0259(16)		
Cu1–Cu2	2.7540(6)		

5.5. 5-Cu-ClO_4

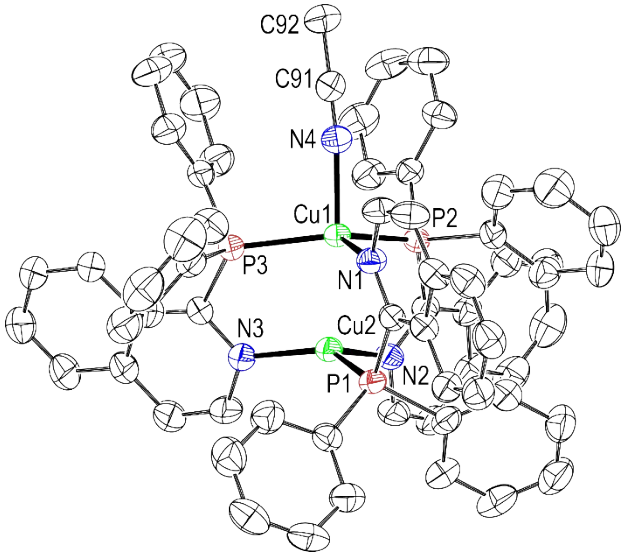

Selected distances Selected angles

Atoms	Distance (Å)	Atoms	Bond Angle (°)
Cu1–N4	2.0412(18)	Cu1–N4 – C91	164.42 (17)
N4–C91	1.142(3)	N4–C91–C92	179.2(2)
Cu1–N1	2.1420(19)		
Cu1–P2	2.2867(9)		
Cu1–P3	2.2800(6)		
Cu2–P1	2.1950(11)		
Cu2–N2	2.0443(19)		
Cu2–N3	2.0061(18)		
Cu1–Cu2	2.5326(5)		

Figure S 53

5.6. 1-Cu-NDMA

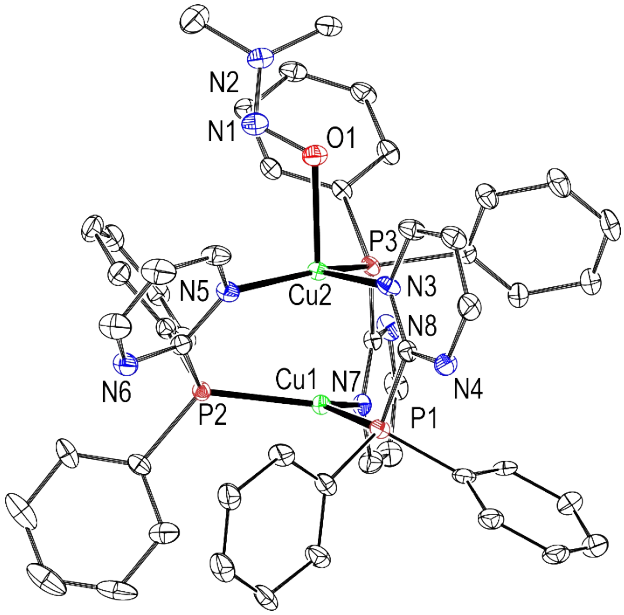

Selected distances Selected angles

Atoms	Distance (Å)	Atoms	Bond Angle (°)
Cu1–N4	2.0412(18)	Cu1–N4 – C91	164.42 (17)
N4–C91	1.142(3)	N4–C91–C92	179.2(2)
Cu1–N1	2.1420(19)		
Cu1–P2	2.2867(9)		
Cu1–P3	2.2800(6)		
Cu2–P1	2.1950(11)		
Cu2–N2	2.0443(19)		
Cu2–N3	2.0061(18)		
Cu1–Cu2	2.5326(5)		

Figure S 54

5.7. 4-Cu-NDMA

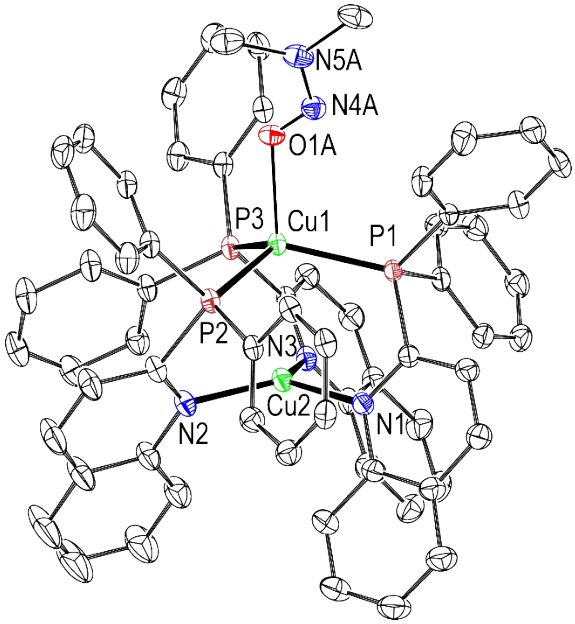

Selected distances

Atoms	Distance (Å)
Cu1–O1A	2.189(16)
O1A–N4A	1.05(2)
N4A–N5A	1.282(10)
Cu1–P1	2.3124(5)
Cu1–P2	2.3142(6)
Cu1–P3	2.3121(7)
Cu2–N1	2.0398(14)
Cu2–N2	2.0249(13)
Cu2–N3	2.0259(13)
Cu1–Cu2	2.7442(6)

Selected angles

Atoms	Bond Angle (°)
Cu1–O1A–N4A	123.4(14)
O1A–N4A–N5A	116.2(12)

Figure S 55

5.8. 5-Cu-II

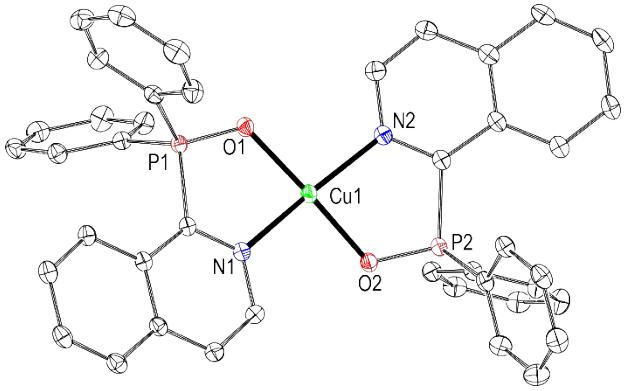

Selected distances

Atoms	Distance (Å)
Cu1–O1	1.9450(13)
Cu1–O2	1.9366(13)
Cu1–N1	1.9986(14)
Cu1–N2	2.0074(14)

Selected angles and torsions

Atoms	Bond Angle/Torsion (°)
O1–Cu1–N1	86.36(6)
O2–Cu1–N2	86.12(6)
O1–N1–O2–N2	14.24(6)

Figure S 56

5.9. 5-Cu-II-NDMA

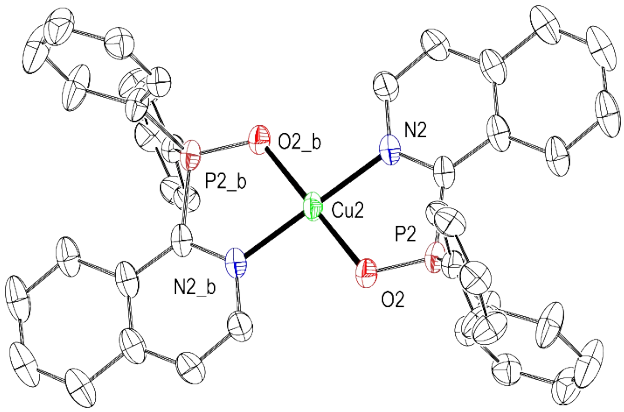

Selected distances

Atoms	Distance (Å)
Cu2–O2	1.9364(15)
Cu2–O2_b	1.9364(15)
Cu2–N2	1.9968(18)
Cu2–N2_b	1.9968(18)

Selected angles

Atoms	Bond Angle/Torsion (°)
O2–Cu2–N2	86.32(7)
O2_b–Cu2–N2_b	86.32(7)
O2–N2–O2_b–N2_2	0.00(7)

Figure S 57

5.10. 3-Cu-NDMA

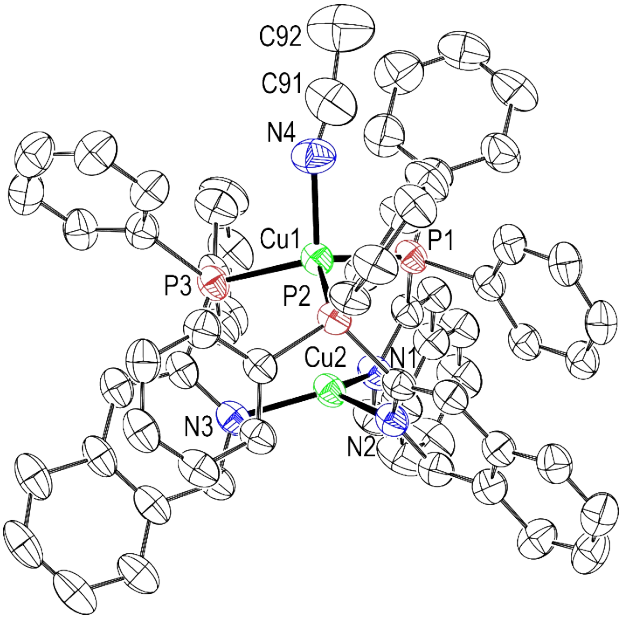

Figure S 58

Selected distance | Selected angles

Atoms	Distance (Å)	Atoms	Bond Angle (°)
Cu1–P1	2.3260(14)	Cu1–N4–C91	155.4(6)
Cu1–P2	2.3091(15)	N4–C91–C92	169.7(10)
Cu1–P3	2.3044(15)		
Cu2–N1	1.989(4)		
Cu2–N2	2.000(4)		
Cu2–N3	1.978(4)		
Cu1–N4	2.051(5)		
Cu1–Cu2	2.7524(11)		

5.11. 5-Cu-ClO_4-NDMA

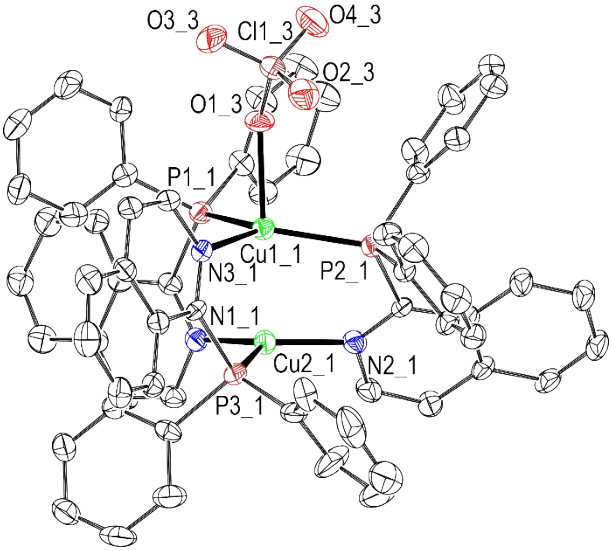

Figure S 59

Selected distances | Selected angles

Atoms	Distance (Å)	Atoms	Bond Angle (°)
Cu1_1–P1_1	2.2928(17)	Cu1_1–O1_3–Cl1_3	143.5(3)
Cu1_1–P2_1	2.2596(17)		
Cu1_1–N3_1	2.082(4)		
Cu2_1–N1_1	2.035(5)		
Cu2_1–N2_1	1.999(5)		
Cu2_1–P3_1	2.2119(18)		
Cu1_1–O1_3	2.227(4)		
Cu1_1–Cu2_1	2.5209(12)		

6. Emission and EPR spectra

6.1. X-ray Photoelectron Spectroscopy characterization on 2-Cu

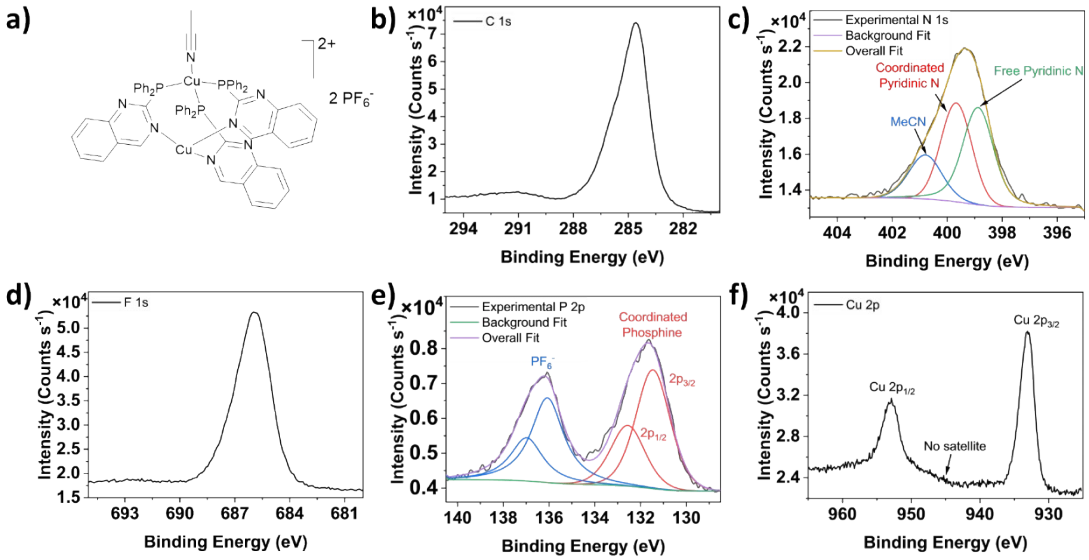

Figure S 60: (a) Proposed solid state structure of 2-Cu. (b) C 1s spectrum. (c) N 1s spectrum with fitting for uncoordinated/coordinated N to Cu(I) as well as the MeCN ligand. (d) F 1s spectrum. (e) P 2p spectrum with fitting for the coordinated phosphines and PF_6^- counterions. (f) Cu 2p spectrum.

6.2. Emission spectrum of phosphine 5 vs phosphine oxide 5-O

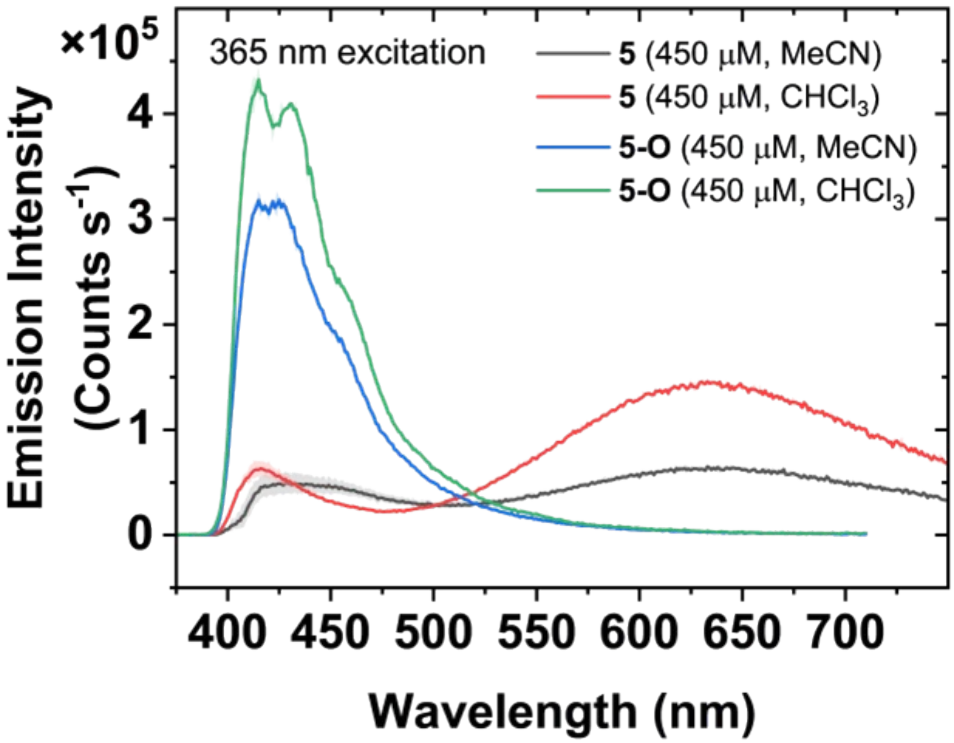

Figure S 61: Emission spectrum (λ_{ex} = 365 nm) of **5** and **5-O** in chloroform and acetonitrile solution under ambient conditions at identical concentrations (450 µM). Background subtraction was performed during data acquisition to remove the Raman scattering signal (≈ 410 nm) from residual water in the solvents.

6.3. Effect of vacuum treatment on 5-Cu-PF_6

^{1}H NMR (400 MHz, $CDCl_3$)

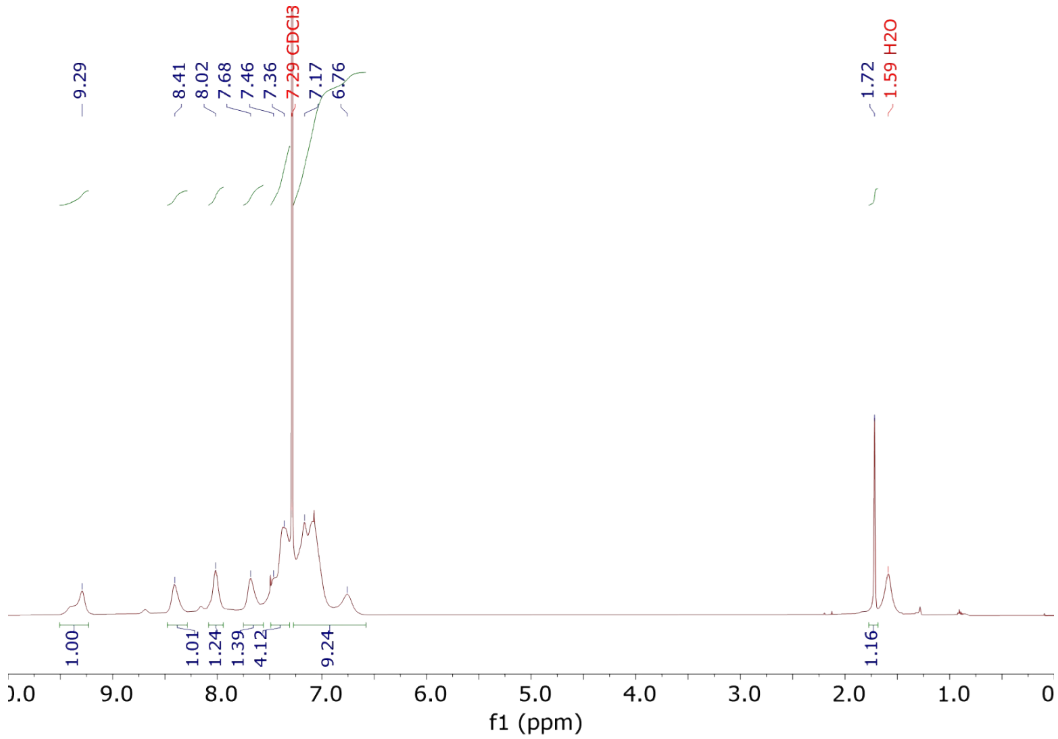

Figure S 62. ^{1}H NMR spectrum of powder **5-Cu-PF_6** sample that is not vacuum treated. The signal at 1.72 ppm may be assigned to coordinated MeCN ligand.

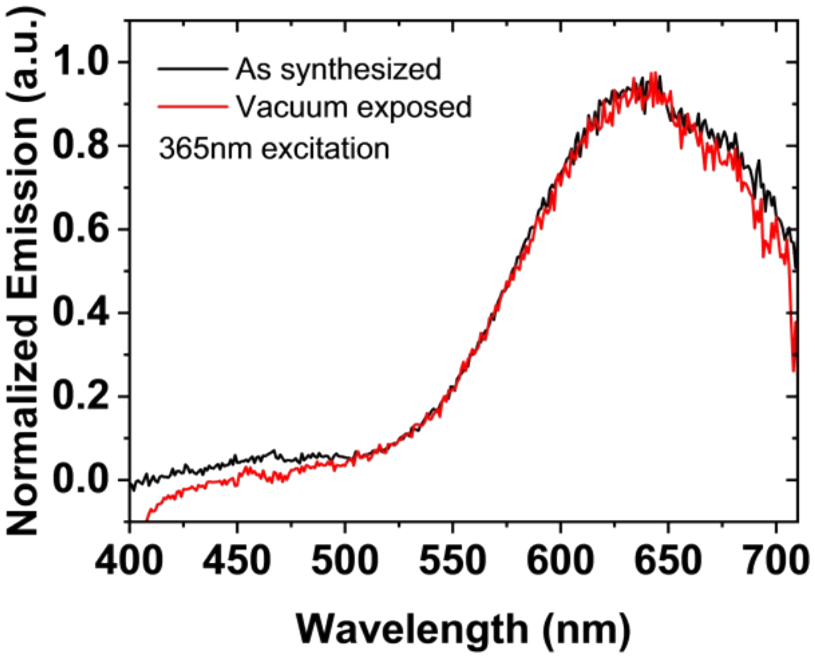

Figure S 63. Solid state emission spectra (λ_{ex} = 365 nm) of **5-Cu-PF_6** as a yellow powder (black trace) and as a neat film after dissolving in $CHCl_3$, dropcasting onto a quartz cover slip and drying in vacuo for 15 min (red trace). Both spectra appear identical.

6.4. Emission quenching of different complexes in solution by NDBA

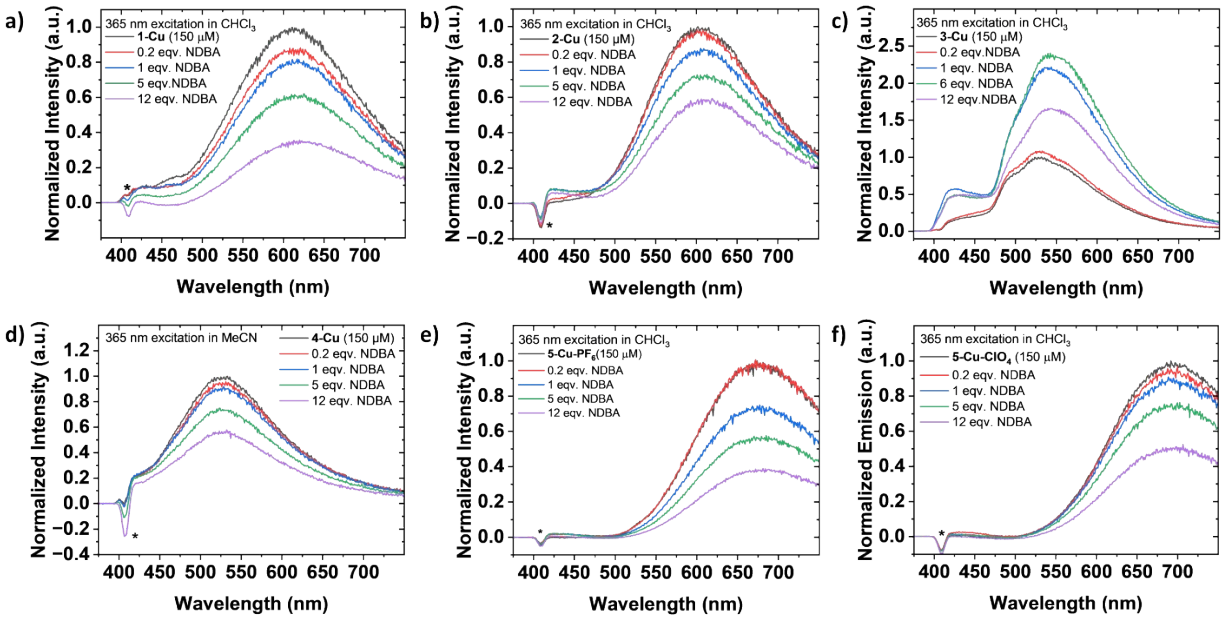

Figure S 64. Emission quenching of copper (I) complexes in chloroform/acetonitrile solution when exposed to various concentrations of *N*-nitrosodibutylamine (NDBA). (a) **1-Cu**; (b) **2-Cu**; (c) **3-Cu**; (d) **4-Cu**; (e) **5-Cu-PF$_6$**; (f) **5-Cu-ClO$_4$**. Data is normalized relative to the trace at 0 equivalents NDBA. The asterisk (*) indicates the location of the Raman scattering signal from residual water in the solvent after background subtraction.

6.5. Different degrees of quenching by NDBA and DBA on 4-Cu

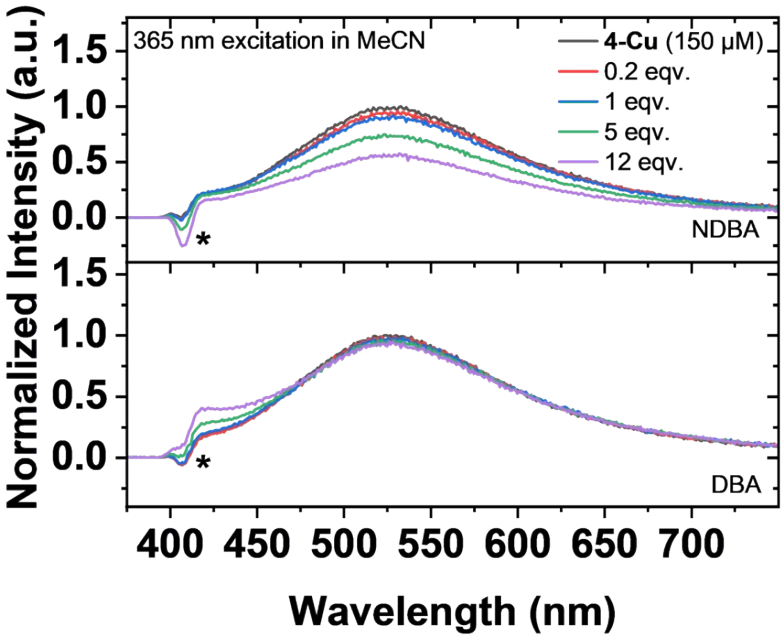

Figure S 65 Comparison of emission spectra of **4-Cu** when exposed to different amounts of Nnitrosodibutylamine (NDBA, top) and dibutylamine (DBA, bottom) in acetonitrile solution. DBA gives negligible quenching of **4-Cu** when compared to NDBA. The asterisk (*) indicates the location of Raman scattering signal from residual water present in the solvent after background subtraction.

6.6. Titration of 3-Cu with different equivalents of NDBA

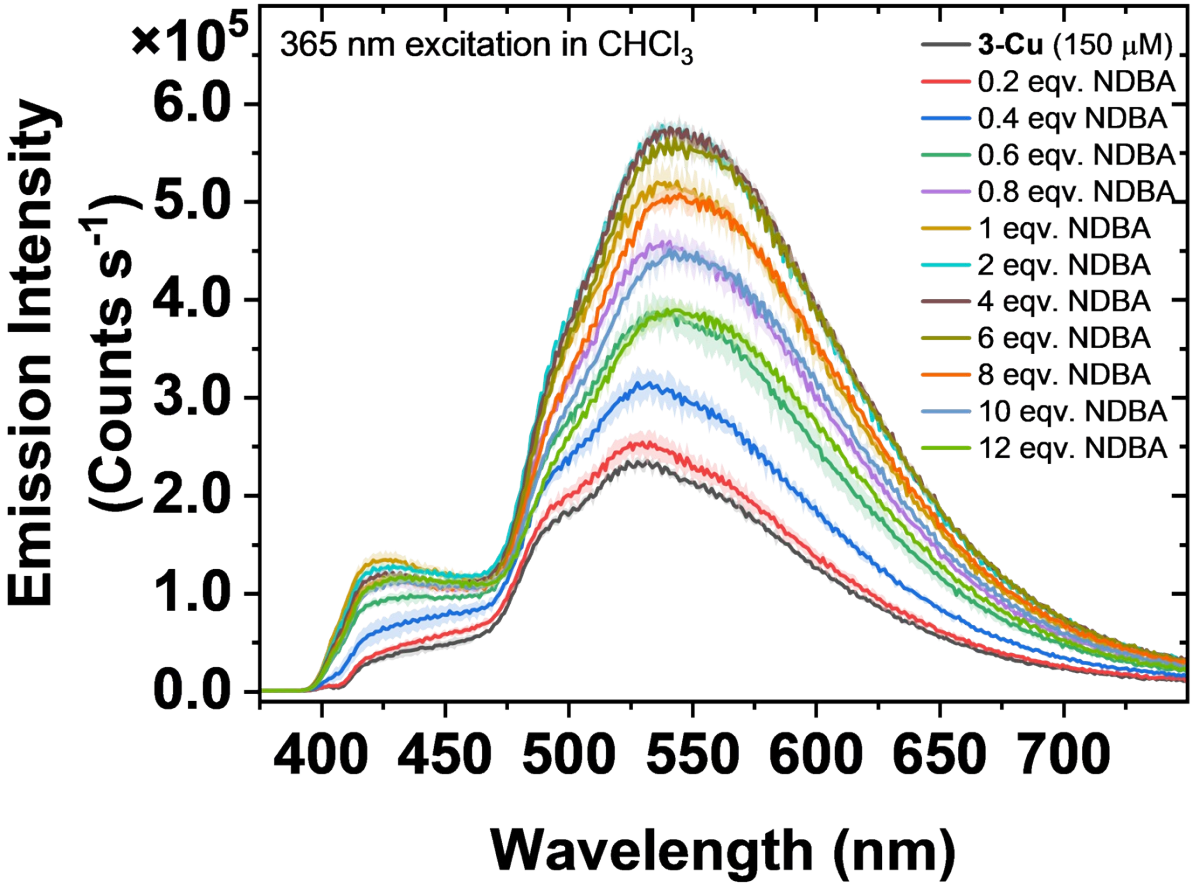

Figure S 66 Changes in emission spectra of **3-Cu** in $CHCl_3$ with increasing equivalents of NDBA. The emission profile increases in emission intensity up to 4 equivalents before further addition of NDBA quenches its emission. The shaded areas around the traces indicate one standard deviation from the averaged data.

6.7. Stern-Volmer analysis on Cu(I) complexes.

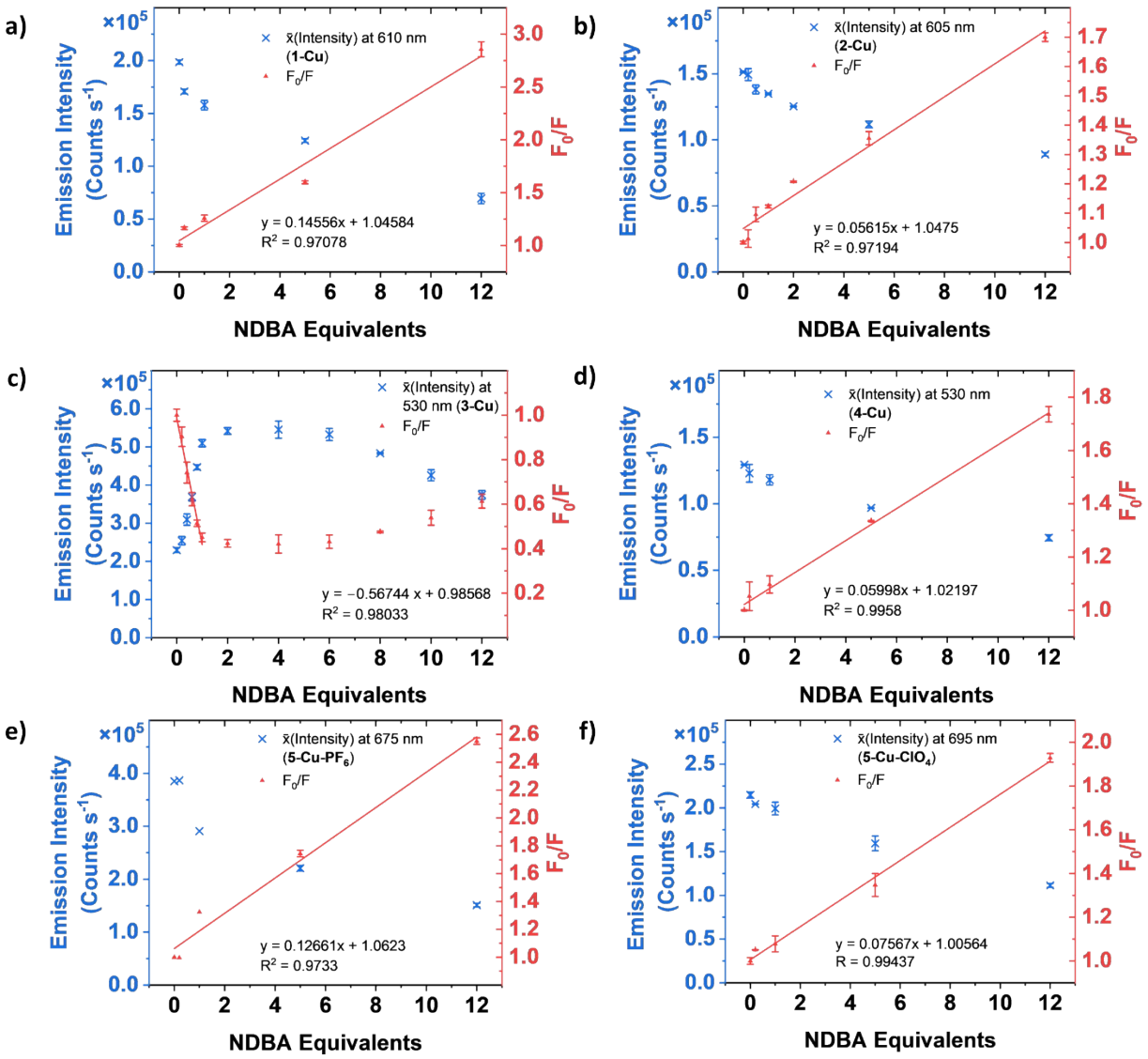

Figure S 67 (a) **1-Cu** in $CHCl_3$; (b) **2-Cu** in $CHCl_3$; (c) **3-Cu** in $CHCl_3$; (d) **4-Cu** in MeCN; (e) **5-Cu-PF$_6$** in $CHCl_3$; (f) **5-Cu-ClO$_4$** in $CHCl_3$. The excitation wavelength was 365 nm in all cases. Fitting was performed on normalized emission values (F_0/F). Error bars indicate one standard deviation away from the averaged data.

6.8. EPR measurements on 5-Cu-II and 5-Cu-ClO_4

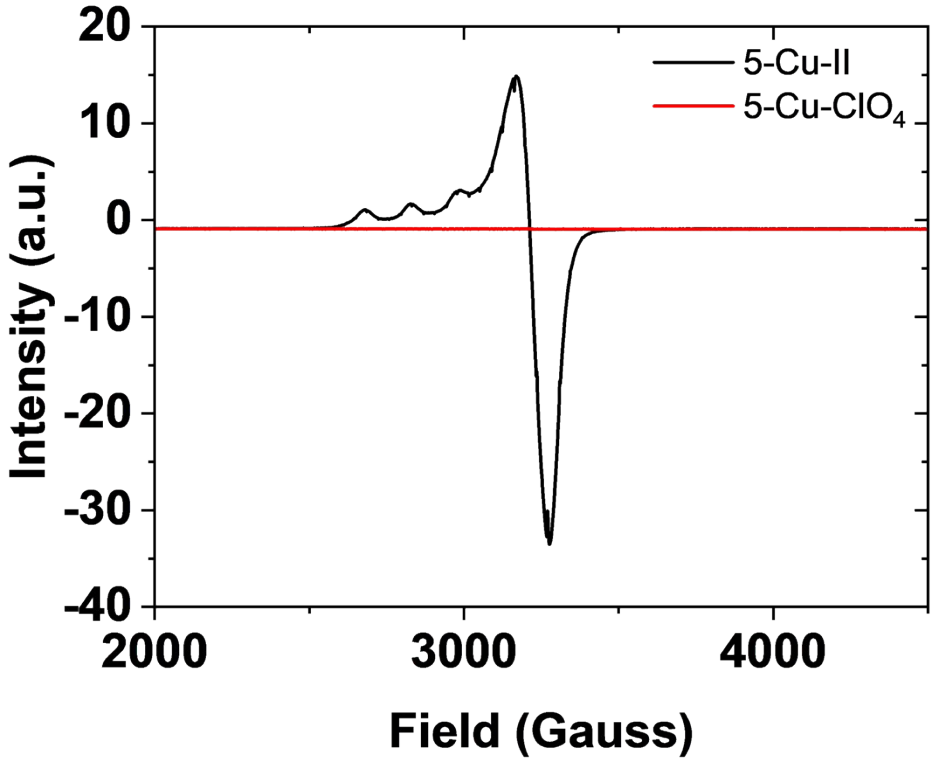

Figure S 68 The copper (II) complex (**5-Cu-II**) shows an axial EPR signal where $g_x = g_y \neq g_z$ often seen for Cu^{2+},[2] whereas the copper (I) complex (**5-Cu-ClO_4**) has no detectable signal.

6.9. Absorption coefficients of copper complexes in this study

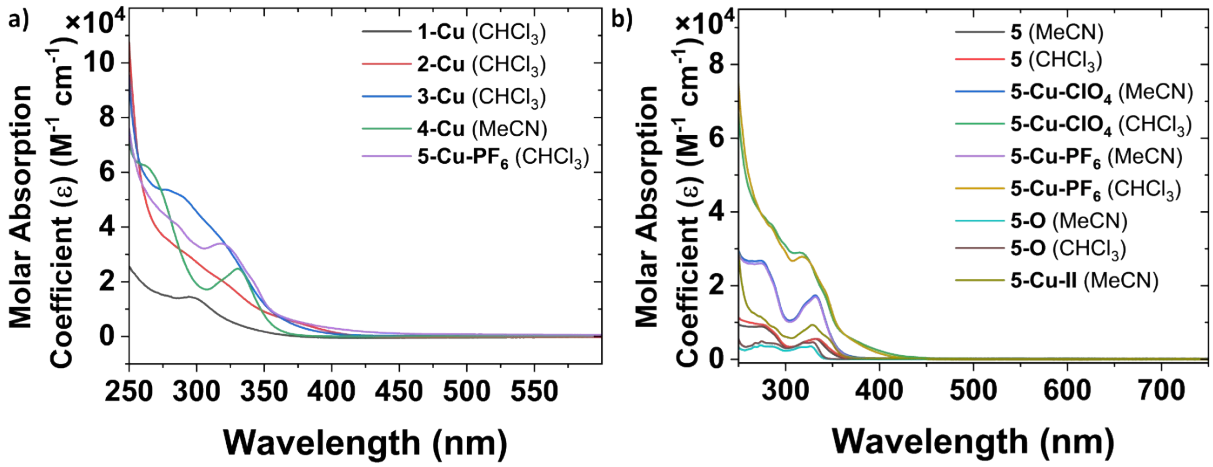

Figure S 69 Molar absorption coefficients (ε) of (a) **1 – 4 Cu** and **5-Cu-PF_6** between 250 and 600 nm in solution. (b) Molar absorption coefficients of **5**, **5-Cu-ClO_4**, **5-Cu-PF_6**, **5-O** and **5-Cu-II** between 250 and 750 nm in solution when investigating the influence of anion, solvent and copper oxidation states.

6.10. Excitation spectra of 5-O and 5-Cu-II

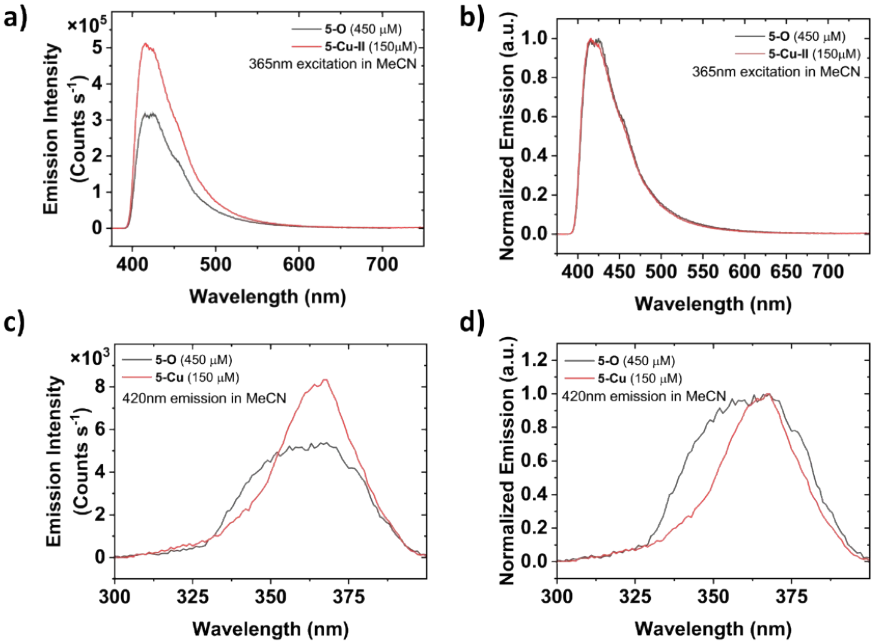

Figure S 70. Top: Emission spectra (λ_{ex} = 365nm) of 5-O and 5-Cu (a) before and (b) after normalization. Bottom: Excitation spectra (λ_{em} = 420 nm) of 5-O and 5-Cu-II (c) before and (d) after normalization. Measurements were carried out in MeCN solution. Displayed spectra have been background subtracted against a solvent only MeCN reference. Sample concentrations used are shown in parentheses.

7. References

1 G. L. Long and J. D. Winefordner, *Anal. Chem.*, 1983, **55**, 712A-724A.

2 G. Pilloni, G. Valle, C. Corvaja, B. Longato and B. Corain, *Inorg. Chem.*, 1995, **34**, 5910–5918.